separations

MDPI

Review

Recent Advances in Using Adsorbent Derived from Agricultural Waste for Antibiotics and Non-Steroidal Anti-Inflammatory Wastewater Treatment: A Review

Abu Hassan Nordin [1,2], Abdul Samad Norfarhana [1,3], Siti Fadilla Md Noor [1], Syafikah Huda Paiman [1], Muhammad Luqman Nordin [4,*], Siti Muhamad Nur Husna [2], Rushdan Ahmad Ilyas [1,5], Norzita Ngadi [1,*], Aznizam Abu Bakar [1], Zuliahani Ahmad [2], Mohammad Saifulddin Azami [2], Wan Izhan Nawawi [2] and Walid Nabgan [6]

1 Faculty of Chemical and Energy Engineering, Universiti Teknologi Malaysia (UTM), Skudai 81310, Johor, Malaysia; abuhassannordin@gmail.com (A.H.N.)
2 Faculty of Applied Sciences, Universiti Teknologi MARA (UiTM), Arau 02600, Perlis, Malaysia
3 Department of Petrochemical Engineering, Politeknik Tun Syed Nasir Syed Ismail, Pagoh Education Hub, Pagoh Muar 84600, Johor, Malaysia
4 Department of Clinical Studies, Faculty of Veterinary Medicine, Universiti Malaysia Kelantan, Pengkalan Chepa, Kota Bharu 16100, Kelantan, Malaysia
5 Centre for Advanced Composite Materials (CACM), Universiti Teknologi Malaysia (UTM), Skudai 81310, Johor, Malaysia
6 Departament d'Enginyeria Química, Universitat Rovira I Virgili, Av. Països Catalans 26, 43007 Tarragona, Spain; wnabgan@gmail.com
* Correspondence: luqman.n@umk.edu.my (M.L.N.); norzita@cheme.utm.my (N.N.)

Abstract: Antibiotics and non-steroidal anti-inflammatory drugs (NSAIDs) are among the top pharmaceutical contaminants that have been often found in the aquatic environment. The presence of these contaminants in the aquatic environment is of great concern since it has a negative impact on both ecology and human health. In contrast to other tertiary treatments, adsorption stands out as a viable treatment approach since it provides benefits such as easier operating conditions with no byproduct formation. Commercial activated carbon is widely researched as a pharmaceutical adsorbent, but its large-scale applicability is constrained by its high cost. Agricultural waste also contains a large amount of various functional groups, which may be adapted to surface modification to increase its adsorption ability. In this regard, this study is designed to review the recent progress of efficient adsorbents derived from various agricultural wastes for the removal of antibiotics and NSAIDs contaminants from water bodies. Adsorbents made from agricultural waste have important benefits over commercial activated carbon for the reduction in waste while controlling water pollution.

Keywords: adsorption; antibiotics; non-steroidal anti-inflammatory drugs; agricultural waste; wastewater treatment

Citation: Nordin, A.H.; Norfarhana, A.S.; Noor, S.F.M.; Paiman, S.H.; Nordin, M.L.; Husna, S.M.N.; Ilyas, R.A.; Ngadi, N.; Bakar, A.A.; Ahmad, Z.; et al. Recent Advances in Using Adsorbent Derived from Agricultural Waste for Antibiotics and Non-Steroidal Anti-Inflammatory Wastewater Treatment: A Review. *Separations* **2023**, *10*, 300. https://doi.org/10.3390/separations10050300

Academic Editors: Sílvia Santos and Ariana Pintor

Received: 28 February 2023
Revised: 24 April 2023
Accepted: 5 May 2023
Published: 8 May 2023

1. Introduction

Pharmaceuticals or medications are chemical substances that are used to treat human and animal ailments. In recent decades, pharmaceuticals, especially antibiotics and non-steroidal anti-inflammatory drugs (NSAIDs) have attracted significant interest because of their huge usage by humans and animals; consequently, they have been detected worldwide in many water bodies [1]. Antibiotics are often used to treat, diagnose, and prevent diseases in humans, veterinary animals, and the agricultural sector [2]. Additionally, NSAIDs are often used to treat a variety of conditions, including gout, arthritis, fever, headaches, and inflammation. Consequently, these pollutants may be noticed in large quantities in surface and groundwater, wastewater, and even drinking water [1,3]. Antibiotic and NSAID pollution in the aquatic environment creates major health problems, which may result in

the development of drug resistance and decreased therapeutic effectiveness [4]. Many studies have shown that for the purpose of removing these contaminants from the aqueous medium, an advanced treatment technique, such as ozonation [5], advanced oxidation [6], electron–Fenton [7], photocatalytic [8], and adsorption [9,10], must be included in the wastewater treatment process.

Among them, adsorption is the most appealing technology due to its inexpensive cost, easy design and scaling-up, simplicity, and high efficiency. A variety of adsorbent materials have been used in wastewater treatment applications, such as natural polymers [11], synthetic polymers [12], biomass [13], and non-commercial materials, including the waste from agricultural sources [14,15]. In recent years, the capability of agricultural waste adsorbents to remove various types of contaminants is attracting attention in the water treatment process. Recycling waste to enhance the adsorption of pharmaceutical complex from water is a green technology that creates a sustainable and closed blue–green cycle. Crop stalks and animal dung are the major types of agricultural waste, which come from our daily lives. Agricultural wastes are lignocellulosic materials with lignin, cellulose, and hemicellulose as their principal structural constituents [16]. Figure 1 shows the chemical composition of some typical agriculture waste [17–25]. These wastes are suitable for use as raw materials to create activated carbon (AC) or adsorbents that undergo surface modification because they include significant amounts of cellulose, hemicelluloses, lignin, lipids, proteins, starch, and other functional groups. In addition, the porosity and voids in the structure of these materials enable tiny compounds, such as NSAIDs and antibiotics, to be trapped. Figure 2 illustrates the sources of antibiotics and NSAIDs pollution that are treated by using adsorbents made from agricultural waste.

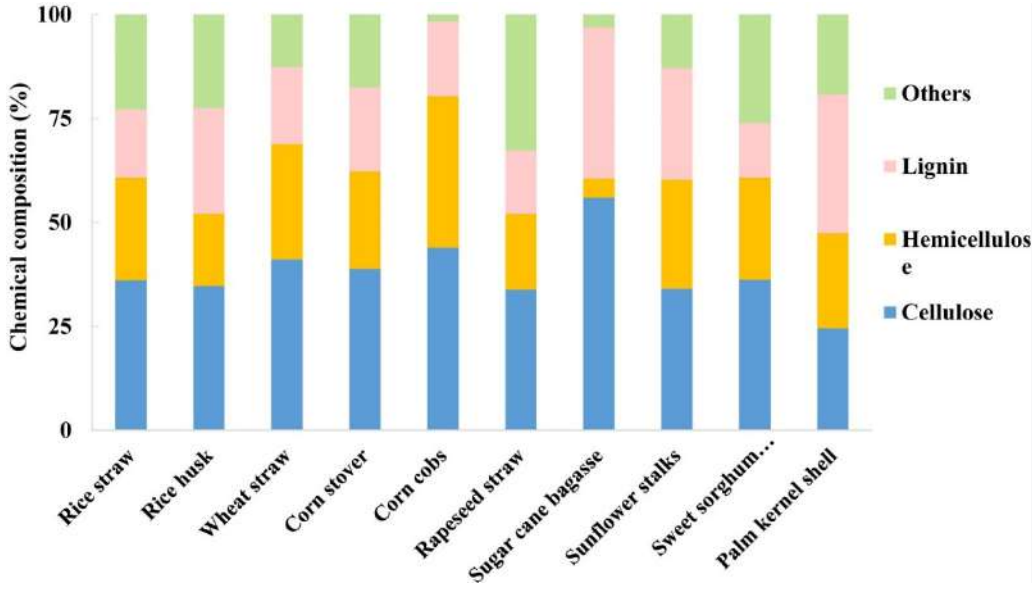

Figure 1. Composition of common agriculture waste [17].

Earlier investigations have focused on the general existence, distribution, and removal of these pharmaceuticals. Moreover, prior evaluations did not emphasize the use of inexpensive substances as pharmaceutical adsorbents, particularly those produced from waste sources. Despite the fact that several works have been publicly available reviewing the utilization of agricultural waste in wastewater treatment applications, there is still a lack of information containing a detailed discussion on the removal of pollutants from the antibiotics and NSAIDs classes. Therefore, this review aims to focus on the current development of adsorption technology synthesized from various agricultural wastes for the removal of antibiotics (e.g., tetracycline, amoxicillin, norfloxacin, chloramphenicol, and sulfanilamide) and NSAIDs (e.g., diclofenac, ibuprofen, aspirin, ketoprofen, and naproxen) from water bodies. This work also discusses the adsorption mechanism for antibiotics and

NSAIDs by agricultural waste adsorbents. It is essential to present an updated and focused review that summarizes the adsorption performance of waste-produced adsorbents for pharmaceutical pollutants removal. This will advance the development of wastewater decontamination using green and imperishable adsorbents.

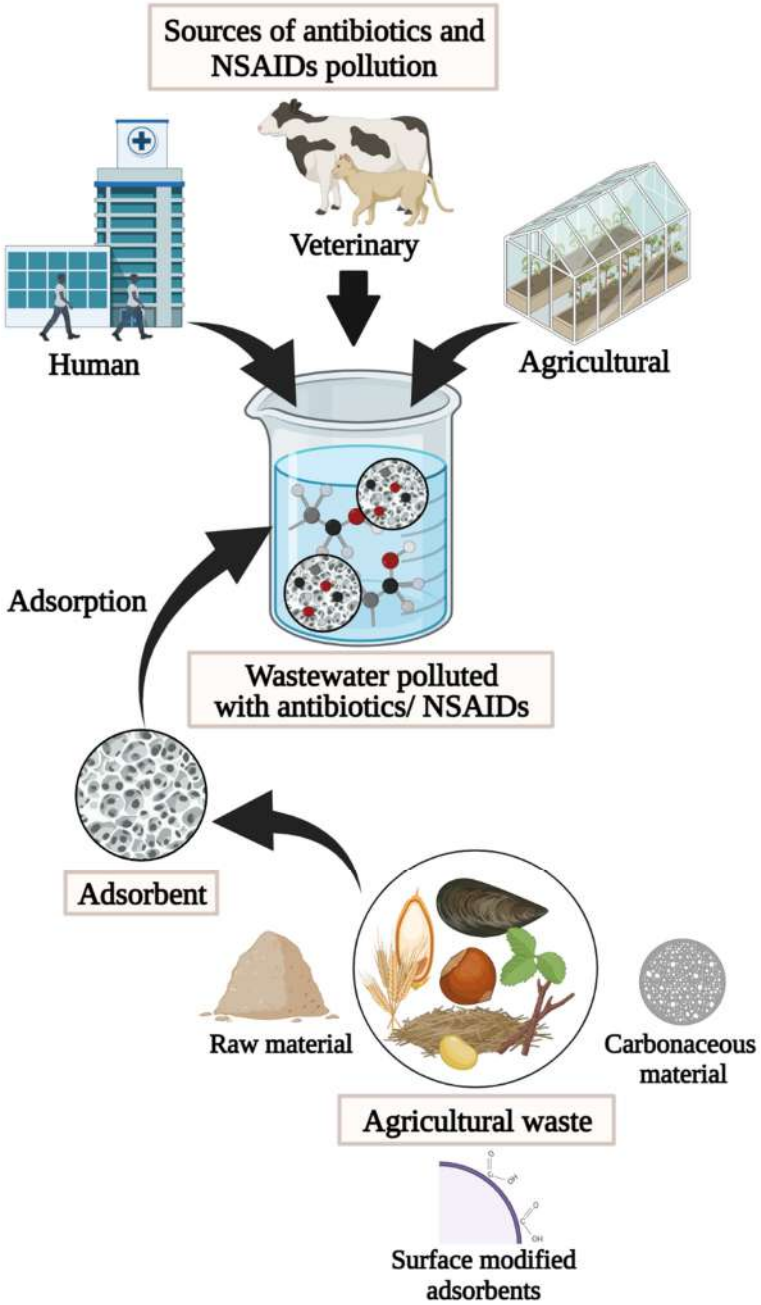

Figure 2. Illustration showing the sources of antibiotics and NSAIDs pollution in wastewater that are derived from human usage, veterinary, and agricultural industries. Wastewater treatment can be performed by using adsorbents made from various agricultural wastes in the form of raw materials, carbonaceous material, or adsorbents that undergo surface modification.

2. The Adsorption of Antibiotics

2.1. Tetracycline

Tetracyclines (TCs) come from different species of *Streptomyces*, and there are twenty compounds that are used as antibiotics [26,27]. TCs are the antibiotics used most in the livestock and aquaculture industries as vaccines or animal feed additives because they are

inexpensive and work well [26–29]. Even though TCs have some benefits for human and animal health, too much can cause allergies in humans, bacterial resistance, and big changes in the microflora of the environment that appear to be bad for ecosystem quality [26,30]. It is difficult to decompose or eliminate them through degradation processes due to bacterial resistance, and their introduction to water bodies sets a major threat to human wellbeing [30]. Membrane filtration, photocatalytic degradation, treatment using electrochemically sophisticated oxidation, and adsorption are some of the non-biodegradable technologies that are investigated to remove TCs from polluted water [4,31]. Among these, adsorption by agricultural waste-based adsorbents has emerged as a prominent technique in practical engineering owing to its advantages such as combination of low-cost, straightforward, and high removal capacity for both organic and inorganic contaminants [32,33].

Zhang, He, Hu, Zhang, Chen, and Xue [30] investigated the production of crayfish shell biochar (BC) at 400, 600, and 800 °C pyrolysis temperature for TC removal. Findings showed that ball milling increased the adsorption performance (39.1 mg/g for CFS800 and 60.7 mg/g for BCFS800), mostly by enhancing the structural properties of the BC. The main mechanism that TCs adsorbed onto BC was through physisorption, which involved filling the pores. This went along with chemisorption, which included hydroxyl complexation, H-bonding, and electrostatic interaction. The BC also exhibited superior recyclability and environmental flexibility, demonstrating its huge application ability for the treatment of TC-laden wastewater.

Hao, Chen, Zhang, and You [29] produced zero-valent iron ZVI-BC from hazelnut shells with excellent adsorption capacity of 39.1 mg/g. pH-dependent adsorption was detected, and the quantities adsorbed were substantial and stable at pH 6–7. The Langmuir and PSO models reasonably matched adsorption data, whereas equilibrium was reached after 40 min. Additionally, Wang et al. [34] synthesized a BC from the modification of Chinese herbal medicine waste (*Flueggea suffruticosa*) with $ZnCl_2$ (Zn-BC), which can remove TC from water by attraction. The pseudo-second-order kinetic equation can describe the adsorption process, and Langmuir's model shows that TCs can adsorb up to 188.7 mg/g at 30 °C. Adsorption happened naturally and could be manipulated by hydrogen bonding and electrostatic contact. The authors reported that Zn-BC possesses a high adsorption capability for TCs over a broad pH and ionic intensity range.

Hoslett et al. [35] used food scraps and plant trimmings to generate BC using a heat pipe reactor. BC has an adsorption capacity for TCs of 9.45 mg/g observed in experimental circumstances. The kinetic models were fitted in the following order: Elovich > PSO > PFO, demonstrating that chemisorption, intraparticle diffusion, and liquid film diffusion all play a role in regulating tetracycline adsorption. Results indicated that the Freundlich isotherm best described the data, pointing to a heterogeneous adsorbent.

Liu, Shao, Wang, Liu, Wang, Gao, and Dai [28] produced pristine BC using an agricultural waste, shiitake mushroom bran, pyrolyzed at 300, 500, and 700 °C to eliminate TCs from water. The Langmuir isothermal adsorption model is followed by the PBC300 and PBC500, whereas the Freundlich model is much easily accommodated by the PBC700. The Langmuir isotherm model revealed that the highest saturated adsorption capacities of PBC300, PBC500, and PBC700 for TCs were 7.568, 14.9944, and 17.68 mg/g, respectively. Pseudo-second-order kinetic models might well explain the adsorption mechanism of TCs, revealing that chemical adsorption was predominant.

Lu et al. [36] examined the opportunity for using a renewable, non-sintered adsorbent by incorporating Fe (III) into bamboo CNFs and then using that material for removal of TCs (TC, CTC, and OTC) from water. Adsorbents modified with Fe (III) exhibited a distinct and rough pore shape and a shift in physicochemical characteristics. The highest adsorption capacities of Fe (III)@CNFs for TC (294.12 mg/g), CTC (232.56 mg/g), and OTC (500.00 mg/g) were demonstrated by fitting data from kinetics, isotherms, and thermodynamics. Possible adsorption processes for TCs onto Fe (III)@CNFs included inner spherical surface complexation, hydrogen bonding, electrostatic contact, and van der Waals forces between both the functional groups of TCs and Fe (III)@CNFs.

Tomczyk and Szewczuk-Karpisz [37] modified sunflower husk BC by adding vitamin C, hydrogen peroxide, or silver nanoparticles, and then studied the effect that this approach had on the BC's porous structure, surface properties, and TC removal capacity. The results demonstrated that the BC modified with vitamin C (BCV) had the greatest potential to attract antibiotic molecules, resulting in the greatest amount of TC adsorption on its surface. It was found that 7.47 mg/g of TC was adsorbed by BCV, 8.41 mg/g by BCH, and 9.55 mg/g by BCV with added silver nanoparticles (BCA). Adsorption was found to be 34.17% (6.83 mg/g) for unmodified BC. The reported data suggest that the enhanced BCs may have been able to increase TC removal from water sources such as groundwater.

Qin et al. [38] made a porous BC from recycled agricultural waste rape straw by carbonizing it at high temperatures and then activating it with potassium hydroxide (KOH) to adsorb TC hydrochloride. The results indicated that KOH-activated BC possessed graphite-like structures, more oxygen-containing functional groups, and a greater specific surface area than inactivated BC, which were beneficial for the TC adsorption. The pseudo-second-order kinetic model and the Freundlich isothermal model were able to provide a good fit to the adsorption data. The mechanism of TC adsorption through KOH activation BC played a part in pore filling, π-π electron donor–acceptor interaction, hydrogen bonding, and electrostatic action. Table 1 summarizes agricultural waste adsorbents used for TC removal.

Table 1. Agricultural waste adsorbent used for tetracycline removal.

Agricultural Waste Adsorbent	Methods/Technique	Adsorption Capacity (mg/g)	Mechanism	Remarks	Ref.
Crayfish shell	Pyrolysis, ball milled	CFS800 = 39.1 BCFS800 = 60.7	• Physical absorption via pore filling • Chemical absorption via hydroxyl complexation, H-bonding, and electrostatic interaction	Adsorption capacity of crayfish shell BC was enhanced, up to 1.5 times by modification via ball-milling method	[30]
Hazelnut shell	Pyrolytic reduction: zero-valent iron@ BC	39.1	• Langmuir and pseudo-second-order models • Spontaneous and endothermic process	The adsorbent possesses high adsorption capacity for other classes of TCs, including oxytetracycline (52.7 mg/g) and chlortetracycline (42.5 mg/g)	[29]
Chinese herbs medicine (*Flueggea suffruticosa*) residue	Pyrolysis: Zn-BC	188.7	• Langmuir and pseudo-second-order models • Spontaneous: controlled by hydrogen bonding and electrostatic interaction	Capable to adsorb other classes of TCs, including oxytetracycline (129.9 mg/g) and chlortetracycline (200 mg/g)	[34]
Mixed food scraps and plant trimmings	Pyrolysis	9.45	• Kinetic models followed the order Elovich > PSO > PFO, chemisorption: intraparticle and liquid film diffusion • Freundlich isotherm: heterogeneous	At the chosen experimental pH, there is little electrostatic interaction between the molecules of BC and tetracycline.	[35]

Table 1. *Cont.*

Agricultural Waste Adsorbent	Methods/Technique	Adsorption Capacity (mg/g)	Mechanism	Remarks	Ref.
Shiitake mushroom bran	Pyrolysis	PBC300 = 7.5 PBC500 = 14.9 PBC700 = 17.6	• PBC300 and PBC500: Langmuir isotherm model • PBC700: Freundlich model • Chemisorption dominant	The pyrolysis temperature is the key to boosting adsorption efficiency	[28]
Bamboo cellulose	Mechanical shearing method	294.12	• Spontaneous and endothermic adsorption: monolayer chemical adsorption	Adsorption capacities of other classes of TCs, including oxytetracycline and chlortetracycline are 232.56 and 500 mg/g, respectively	[36]
Sunflower husks	Pyrolysis	BCV = 8.41 BCH = 7.47 BCA = 9.55 BC = 6.83	• Pseudo-second order model • Equilibrium: Redlich–Peterson model.	Insignificant increase in adsorption capacity between modified BCs and unmodified BC	[37]
Rape straw	Pyrolysis, KOH activation	325.07	• Pseudo-second-order kinetic model and Freundlich isothermal model • Endothermic and spontaneous • Pore filling, π-π electron donor–acceptor interaction, hydrogen bonding, and electrostatic action	Regeneration tests revealed that even after six cycle studies, the TC elimination effectiveness could still reach 97.0%.	[38]

2.2. Amoxicillin

Amoxicillin (AMX) is routinely employed as a top pick medication in the treatment of common diseases in both human and animals, making it one of the antibiotics used today [39]. AMX may enter soils and other environment sectors as a contaminant, having the potential to affect environmental quality. To fix or lessen these problems, it would be interesting to devise effective and inexpensive ways to keep or remove this compound [39]. This includes the adsorption process by agricultural waste materials.

Cela-Dablanca, Barreiro, Rodríguez-López, Santás-Miguel, Arias-Estévez, Fernández-Sanjurjo, Álvarez-Rodríguez, and Núñez-Delgado [39] investigated the adsorption/desorption of AMX in various farming soils along with and without the addition of bioadsorbents, which were pine bark, wood ash, and mussel shell. The data demonstrated improved AMX adsorption for all adjustments, but pine bark performed the best. The Freundlich equation offered the top fit between empirical adsorption data and the evaluated adsorption models. Overall, the bioadsorbents investigated helped to maintain AMX in the applied soils, reducing the risk of pollution by AMX, thus become highly valuable and viable to secure sustainability of the environment and global health.

Chakhtouna, Benzeid, Zari, and Bouhfid [2] developed BC from banana pseudo-stem fibers at various temperatures using slow pyrolysis, which was then coated with $CoFe_2O_4$ nanoparticles in situ for AMX removal from wastewater. Experiments on adsorption demonstrated that the hybrid nanocomposite Co-BP350 exhibited the highest effective AMX adsorption over a broad range of pH and temperature, creating a potential medium

for treating wastewater. Using 50 mg at neutral pH and ambient temperature, the adsorption finding achieved 99.99 mg/g maximum capacity. Adsorption rates and isotherms matched the pseudo-second-order and Langmuir models, demonstrating that single-layer adhesion of AMX to magnetic BC is dominated by electrostatic interactions, π-π stacking, and hydrogen bonding. The magnetic BC's exhibit characteristics that remained practically unchanged after five adsorption–desorption cycles, making it a viable adsorbent for removing medicinal substances from wastewater.

Yazidi et al. [40] synthesized durian shell AC, which was examined in single and binary systems for AMX and TC removal. The results obtained showed the adsorption capacity in single system is greater than binary system for both pollutants. Adsorption isotherms demonstrated the maximum adsorption capacity of AMX was greater compared to TCN at all temperatures examined, indicating the capability of this adsorbent to eliminate AMX from the aqueous solution.

Daouda et al. [41] successfully synthesized and optimized an agricultural waste adsorbent made from coconut shell for AMX removal by using the response surface methodology (RSM) with two considerations: the impregnation ratio (IR) and the activation temperature. The AC made from coconut shells showed its best qualities with a significant microporous specific surface (S_{BET} = 437 m^2/g and V_{micro} = 0.21 cm^3/g), optimum iodine adsorption (930.28 mg/g), amorphousness, and a low heterogeneous composition. Excellence physical and chemical properties of the BC occurred at 740 °C in phosphoric acid (IR = 1.66), which resulted in ideal removal of over 98% of AMX. The adsorption procedure fitted the Langmuir isotherm and pseudo-first-order model. The adsorbate–adsorbent proportion was the key limiting factor in adsorption.

Hashemzadeh et al. [42] discovered that carbon nanoparticles derived from aloe vera leaf provided an inexpensive agricultural adsorbent for decontaminating water containing AMX and Cephalexin. The activity of carbon was evaluated using aqueous samples of H_2SO_4 (Av-Sc) and HNO_3 (Av-N-Ac). The findings indicated that the pseudo-second-order kinetic model (R2 > 0.99) and the Langmuir isotherm model (R2 > 0.99) offered a satisfactory fit for the available experimental data. The maximal absorption capacities for AMX in (Av-S-Ac) and (Av-N-Ac) adsorbents were 28.86 and 29.11 mg/g, respectively. Table 2 summarizes the agricultural waste adsorbents used for AMX removal.

Table 2. Agricultural waste adsorbents used for amoxicillin removal.

Agricultural Waste Adsorbent	Methods/Technique	Adsorption Capacity (mg/g)	Mechanism	Remarks	Ref.
Pine bark	Soil amendment mixture	n/a	• Freundlich model	After the bioadsorbent materials were integrated into the soil, AMX desorption declined and reached levels that did not exceed 6%	[39]
Wood ash					
Mussel shell					
Durian Shell	Pulverization, physical activation by CO_2, pyrolysis	n/a	• Parallel and non-parallel orientations • Single and binary systems involved physical interactions	All adsorption capacities declined after transitioning from single to binary systems	[40]

Table 2. *Cont.*

Agricultural Waste Adsorbent	Methods/Technique	Adsorption Capacity (mg/g)	Mechanism	Remarks	Ref.
Banana pseudo-stem	Pyrolysis, co-precipitation, in situ hybrid nanocomposites	99.99	• Adsorption kinetics and isotherms are compatible with pseudo-second-order and Langmuir models • Electrostatic interactions, stacking of π-π, and bonds of hydrogen	After five cycles of adsorption–desorption, the adsorption performance was essentially unchanged	[2]
Coconut shell	Chemical activation process: Pre-treatment, impregnation, carbonization and washing	930.28	• Langmuir isotherm and the pseudo-second-order kinetic model	A high adsorption capacity of the adsorbent is associated with its huge microporous surface area	[41]
Aloe vera leaf waste	Carbonization	26.34	• Pseudo-second-order kinetic model and Langmuir isotherm model	Adsorption interactions are categorized as electron donor–acceptor hydrogen bonding interaction, and hydrogen bonding	[42]

n/a: not applicable.

2.3. Norfloxacin

Norfloxacin (NFX, 1-ethyl-6-fluoro-1, 4-dihydro-4-oxygen-7-(1-piperazinyl)-3-quinoline carboxylic acid) fluoroquinolone compound is mostly used to treat diseases in livestock, animal products, and humans, including urinary tract infections, viral infections, and inflammations [43,44]. NFX is an antibiotic that has been found in recent years at degrees ranging from nanograms per liter (ng/L) to micrograms per liter (g/L) in various marine environments and drinking water [45]. The existence of these components has become a concern as they are resistant to change [46]. Adsorption by agricultural waste has been reported to be a potential technique for the removal of NFX.

For example, different agricultural wastes (peanut shell, maize straw, and soybean straw) and pyrolysis temperatures (300, 450, and 600 °C) were studied to determine their impacts on BC's structural morphology and chemical compositions [43]. The results demonstrated that BC's pH, surface area, and ash composition all improved after heating. The adsorption mechanisms of BC varieties on NFX were compatible with the Langmuir model and pseudo-second-order kinetic model. Adsorption occurred predominantly by chemisorption at the BC's surface.

As shown in research conducted by Nguyen, Nguyen, Dat, Huu, Nguyen, Tran, Bui, Dong, and Bui [46], spent coffee grounds BC (SCGB) may be utilized to effectively remove NFX from water. The spent coffee grounds that were pyrolyzed at 500 °C indicated the maximum removal of NFX and significant specific surface area of the adsorbent (46.32 m^2 g^{-1}). NFX adsorption mechanism of SCGB best fits the Langmuir model (R2 = 0.974) with maximal uptake capacity (69.8 mg/g). Using the response surface method (RSM), the best adsorption conditions were determined to be 6.26 pH, 24.69 mg/L NFX, and 1.50 g/L SCGB.

A new shaddock peel-derived N-doped activated carbon (NAC) was examined for its capacity to eliminate NFX from aqueous solution [44]. The adsorption process was accurately characterized by the pseudo-second-order kinetic model, and the Langmuir and Koble–Corrigan isotherms provided a perfect fit to the equilibrium data. The adsorption of NFX on NAC was significantly governed by hydrophobic effect, π-π electron donor–acceptor (EDA) interaction, electrostatic interaction, hydrogen bonding, and the Lewis

acid–base effect. The maximal single layer adsorption rate for NFX was 746.29 mg/g at 298 K, indicating a viable NAC as an adsorbent for removing NFX from water.

Zhang et al. [47] successfully developed amorphous porous BCs with a large specific surface area (935 m^2 g^{-1}) made from sesame straw. Roughly equivalent to other BCs precursors, sesame straw is less expensive and better for the environment because it has many uses and is easy to find. KOH and $Ca(OH)_2$ acted as co-activators, with characterization findings showing that co-activators had greatly expanded the roughness of BC surface and enhanced porous structure. Pseudo-second-order kinetics and the Sips model accompanied adsorption experiment data, signifying heterogeneous and multi-layer adsorption.

Pyrolyzed waste pomelo peel was conducted at 400 °C to generate BC, which was then employed as an adsorbent to extract NFX from synthetics wastewater (Zhang et al. [48]). The optimized adsorption conditions were at 0.5 g/L, pH 3, and 45 °C; BC's highest adsorption capacity was 3.0272 mg/g. Best-fitting pseudo-second-order kinetics to the adsorption process confirmed the chemical adsorption mechanism. Honeycomb lignin-based BC (HLB), made by hydrothermally activating industrial lignin of corn straw pulp, was used to eliminate NFX from water [49]. The findings of batch adsorption tests demonstrated that HLB has a great capacity to remove NFX over a broad pH range. Pore filling, electrostatic interaction, π-π interaction, and hydrogen bonding all played a role in NFX elimination. In particular, HLB's extremely aromatized structure and the abundance of oxygen-containing functional groups (–OH, C–O, etc.) facilitated π-π interaction. Table 3 summarizes the agricultural waste adsorbents used for NFX removal.

Table 3. Agricultural waste adsorbents used for norfloxacin removal.

Agricultural Waste Adsorbent	Methods/Technique	Adsorption Capacity (mg/g)	Mechanism	Remarks	Ref.
Peanut shell	Pyrolysis	40.15	• Langmuir model and pseudo-second-order kinetic model • Surface layer dominated by chemisorption • Adsorption mechanism: pore filling, hydrogen bonding, and electrostatic interactions	The best pyrolysis temperature of the adsorbent was 600 °C, with highest adsorption performance at temperatures of 300 and 450 °C	[43]
Corn straw		36.28			
Soybean straw		39.19			
Spent coffee grounds	Pyrolysis	69.8	• Langmuir and Freundlich models	The BC prepared by spent tea grounds had better adsorption of NOR than potato stem, willow branches, wheat straw, cauliflower roots, and corn and reed stalks	[46]
Shaddock peel	Hydrothermal carbonization (HTC) pre-treatment	746.29	• Langmuir and Koble–Corrigan isotherms, pseudo-second-order kinetic model • π-π electron donor–acceptor (EDA) interaction, hydrophobic impact, hydrogen bonding, electrostatic interaction, and Lewis acid–base effect	Excellent adsorption performance was associated with high pore and surface area of adsorbent	[44]

Table 3. *Cont.*

Agricultural Waste Adsorbent	Methods/Technique	Adsorption Capacity (mg/g)	Mechanism	Remarks	Ref.
Sesame straw	Pyrolysis	221.37	• Pseudo-second-order kinetics and Sips model (Langmuir–Freundlich) • Heterogeneous and multi-layer • Electrostatic interaction, hydrogen bond, and π-π interaction	High specific surface area and large pore volume of adsorbent contributed to the high adsorption capacity	[47]
Pomelo peel waste	Pyrolysis	3.0272	• Interaction between BC dosage and solution pH was extremely significant on removal efficiency and adsorption capacity • Pseudo-second-order kinetics • Chemical adsorption	The sequence of the most influenced parameters for adsorption were solution pH, BC dosage, and reaction temperature	[48]
Honeycomb lignin-based BC	Hydrothermal carbonization and then KOH activation	529.85	• Langmuir–Freundlich model • Spontaneous and endothermic • Pore filling, π-π stacking, hydrogen bonding, and electrostatic interactions	HLB showed strong selectivity and recycling capabilities; in the presence of competing ions, the removal rate for NOR reached 99.5% and was sustained at least 98% of the time after 12 adsorption cycles	[49]

2.4. Chloramphenicol

Chloramphenicol (CAP) is a wide-ranging antibiotic applied in both human and animal prescription owing to its inexpensive cost and inhibitory efficacy against bacterial diseases such as cholera and typhoid conjunctivitis, including those caused by Gram-negative and typhoid germs [50,51]. While CAP has many positive advantages, its use in both human and animal medicine has also been linked to a number of potentially fatal adverse effects. Plastic anemia, bone marrow failure, and blood disorders are only some of the serious illnesses that may result from prolonged exposure to CAP, which is thought to be a carcinogen. In spite of the carcinogenic and additional detrimental health implications of CAP, the regularity of this antibiotic was identified in various water sources as a consequence of the continued, unregulated, and excessive use of CAP in veterinary medicine [52].

The persistent presence of CAP in marine ecosystems leads to an antibiotic resistance problem. Therefore, an efficient technique to treat waste from CAP in wastewater treatment is needed to be discovered [53]. On the basis of cost, efficiency, and ecological considerations, adsorption has evolved into a cost-efficient and environmentally safe method. However, the formulation and development of recycling waste and effective adsorbents has remained a persistent obstacle [53]. For this reason, it is crucial to produce biosorbents from agricultural wastes that can aid in the elimination of antibiotics.

Chen, Pang, Wei, Chen, and Xie [50] investigated the utilization of porous carbon (PC) materials (i.e., raw material: waste lignin) for the elimination of CAP in water. Maximum capacity of this adsorbent was determined to be 534.0 mg/g at 303 K. The adsorption isotherm was most accurately depicted employing the Langmuir isotherm model and pseudo-second-order kinetics. The study found that the adsorption removal CAP relied on physisorption with chemisorption as a practice complement. Additionally, Wang et al. [54] produced a large surface area and porous structure BCs from several agricultural wastes,

namely *Lycium barbarum L. branches* (LBL), corncob (CC), rice straw (RS), *Zizania latifolia* (Griseb.) *Stapf* (ZLS), and soybean (SB), using a simple pyrolysis and alkaline activation process and assessed their ability to remove CAP from aqueous systems. Physisorption via micropore filling, in contrast to π-π electron donor–acceptor, electrostatic, and hydrophobic interactions, seems to be the predominant adsorption mechanism.

Corn stalk biomass fiber (CF) and Fe_3O_4-embedded chitosan (CS) were used by Xing et al. [55] to create a new biomass-based adsorbent (CFS) to extract CAP from an aqueous phase. Adsorption isotherms from batch tests were perfectly matched by the Langmuir and adsorption kinetic data fit, and the pseudo-second-order kinetic model matched well. On CFS, CAP adsorption took place endothermically, spontaneously, and in an entropy-increasing manner. Furthermore, the CFS may be isolated by an external magnetic field, recycled, and regenerated with no a noticeable reduction in the CAP's absorption capability. Considering these impressive results, CFS presents a good material for the treatment of CAP from the aqueous environment.

Wang, Yong, Luo, Yan, Wong, and Zhou [54] produced AC adsorbents (named CFAC-n) with greater adsorption capacity using coconut fiber carbon and a KOH activator. The adsorption capacity of CFAC-n was significantly correlated with its specific surface area. CFAC-3 (mass ratio of CFAC-1:KOH-3) had the maximum specific surface area (1755 m^2/g) and adsorption capacity (523.0 mg/g). The CAP adsorption onto CFAC-n worked well with both the pseudo-second-order and Elovich kinetic models. These findings demonstrated that the adsorption mechanism was heterogeneous adsorption via primary chemisorption. Adsorption was primarily mediated via hydrogen bond and π–π conjugation interactions, and electrostatic interaction.

Pasta et al. [56] studied cattail leaves and their use for removing the antibiotic CAP from aqueous systems. Results from both the FTIR spectrum and the NMR analysis were consistent, demonstrating the presence of functional chemical groups that facilitate interaction between the biosorbent and the analyte. SEM images revealed that the material took the form of parallel plates with a high channel density (heterogeneous surface). Pseudo-second-order best matched the kinetics model of adsorption, whereas the Freundlich model provided the most accurate estimate of maximal capacity. Table 4 summarizes the agricultural waste adsorbents used for CAP removal.

Table 4. Agricultural waste adsorbents used for chloramphenicol removal.

Agricultural Waste Adsorbent	Methods/Technique	Adsorption Capacity (mg/g)	Mechanism	Remarks	Ref.
Lignin waste	Pyrolysis	534	• Langmuir isotherm model and pseudo-second-order kinetic • Spontaneous and endothermic • Physical and chemical synergistic effects favored the adsorption	The best preparation parameters were: pyrolysis temperature of 800 °C and K_2CO_3/sodium lignosulfonate mass ratio of 4	[50]
Cattail leaves	Muffle pyrolysis	0.0103	• Freundlich isotherm model and pseudo-second-order • Heterogeneous surface that promotes the adsorption of drugs by physisorption	The raw material had a small surface area and was either non-porous or mostly composed of meso- and macropores	[56]

Table 4. *Cont.*

Agricultural Waste Adsorbent	Methods/Technique	Adsorption Capacity (mg/g)	Mechanism	Remarks	Ref.
Lycium barbarum L. branches (LBL)	Low-temperature carbonization (2 h at 400 °C), high-temperature KOH activation (4 h at 800 °C)	436.7	• Langmuir model, a pseudo-first-order rate • A spontaneous adsorption method for CAP • More graphite and tougher hydrophilicity decreased the adsorption capacity • Micropore filling is the leading adsorption mechanism and chemical interactions are engaged during the adsorption process, and they synergistically contribute substantially to the high CAP adsorption capacity	The adsorption capability was reduced by increased hydrophilicity and graphite content	[54]
corncob (CC)		497.5			
rice straw (RS)		469.5			
Zizania latifolia (Griseb.) Stapf (ZLS)		606.1			
Soybean (SB)		892.9			
Corn stalks fiber	Embedded with chitosan and Fe_3O_4	58.75	• Langmuir isotherm model • Pseudo-second-order kinetic model • Endothermic, spontaneous	The adsorbent has a large capacity for reuse and may be used up to five times	[55]
Coconut fiber	Pyrolysis (800 °C for 3 h), KOH activation	523.0	• Pseudo-second-order kinetic and Elovich kinetics model • Freundlich and Temkin isotherm model • Heterogeneous adsorption by main chemisorption • Hydrogen bond and π-π conjugation interactions, and electrostatic interaction	The adsorbent is mostly made of basic functional groups and has a separate microporous and mesoporous network, which both contributed to the adsorption	[57]

2.5. Sulfanilamide

Geng et al. [58] investigated the adsorption of sulfonamide antibiotics using BC derived from walnut shells. The derived BC was functionalized with nitric acid under reflux at a different temperature to introduce BC with more functional groups. The FTIR results clearly showed more functional groups attached together with O–H, C=C, C=O, N=O, O=C–O, and C–O after functionalization. The functional groups help in facilitating the sulfonamide adsorption with the adsorption capacity for three different sulfonamide groups of 32 mg/g (SDZ), 46 mg/g (SDM), and 40 mg/g (SCF).

Xu et al. [59] derived AC from cottonseed husks and tested them for sulfanilamide adsorption. The study first treated the cottonseed husk (CSH) by growing *Pleurotus ostreatus* on the CSH to offer CSH a more porous structure. This enables the chemical activator to enter the CSH matrix during activation and serves to increase the specific surface area. Next, the carbonization step at 500 °C and the activation process using sodium hydroxide (NaOH) at 800 °C produced AC (CSH-AC-0, CSH-AC-40, and CSH-AC-80) with a specific surface area of 3406, 3129, and 2866 m^2/g, respectively. The adsorption study measured the adsorption capacities for sulfanilamide, which were 139.43, 146.15, and 146.16 mg/g for CSH-AC-0, CSH-AC-40, CSH-AC-80, respectively.

Prasannamedha et al. [60] derived BC from sugarcane bagasse and tested it for sulfamethoxazole (SMX) removal. SMX is a group of sulfonamide bacteriostatic antibiotics. The author prepared BC via hydrothermal carbonization (HTC) and followed with an acti-

vation step using NaOH as the chemical activator. This synthesis process produced BC with a specific area of 1099 m^2/g. It has a sphere-like structure augmented with hydrophobic groups inside and hydrophilic groups outside. Therein, the interaction with SMX possesses the derived BC with an adsorption capacity of 400 mg/g.

In addition, Qin et al. [61] had synthesized BC from sugarcane bagasse and tested for four different kinds of sulfanilamide antibiotics (sulfamethoxazole, thiazole, methylpyrimidine, and dimethylpyrimidine). Under the optimum adsorption condition of pH 4, the derived BC at a 500 °C carbonization temperature and activated with 30% hydrogen peroxide possess the antibiotic removal rate of ~89%. Additionally, Aslan and Şirazi [62] investigated the adsorption of sulfadiazine (SDZ), an antibiotic of the sulfonamide group, by using AC derived from olive pomace. At the preparation requirements of 840 °C for the activation temperature and 1:4 impregnation ratio of the KOH activator, AC was derived with the greatest surface area of 2451.770 m^2/g. The maximum adsorption capacity achieved for SDZ is 66.2252 mg/g following the best-fit Langmuir isotherm model.

Weng and Yu [63] prepared BC from coconut shells and modified it with $FeCl_3$ to add magnetic properties to the derived BC for easy adsorbent separation. Despite the magnetic modification showing a slight reduction in specific surface area from 1719 to 1267.3 m^2/g, the magnetic-derived BC possesses a high adsorption capacity, 294.12, 400.00 and 454.55 mg g^{-1}, for three different sulfanilamide groups: sulfadiazine (SDZ), sulfamethazine (SMT), and SMX of, respectively. Another type of BC was prepared by Hu et al. [64], derived from rice husk with attapulgite and studied for removal of SDZ and SMT adsorption. For the synthesis condition at a ratio of 1:10 attapulgite and rice husk, the doped BC (ATP/BC-0.1) produced had the highest specific surface area, 113.75 m^2/g. The ATP/BC-0.1 achieved removal of SDZ and SMT at 98.63% and 98.24%, respectively. Table 5 summarizes the agricultural waste adsorbents used for sulfanilamide removal. Figure 3 represents the summary of agricultural waste from marine products and plants used as adsorbents for antibiotics wastewater treatment.

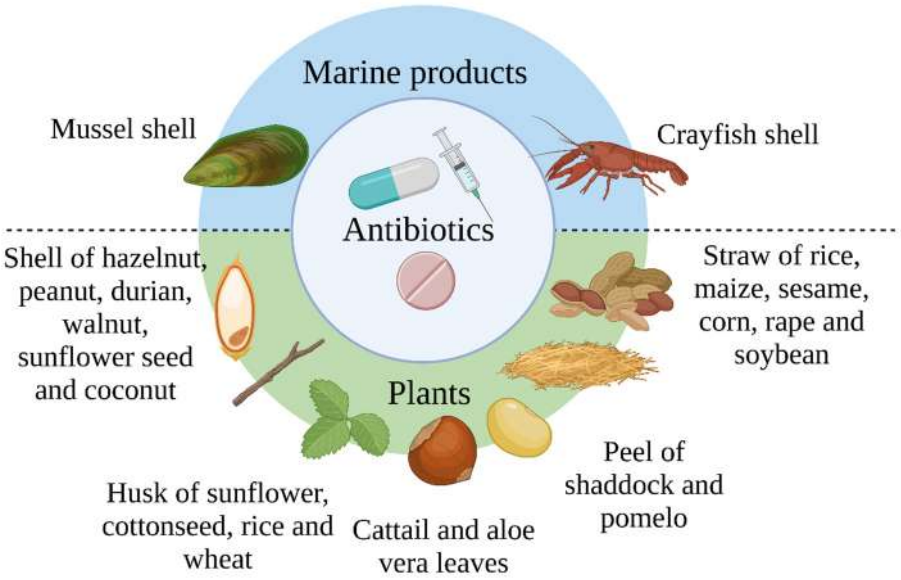

Figure 3. Summary of agricultural waste used as adsorbents for antibiotics wastewater treatment.

Table 5. Agricultural waste adsorbents used for sulfanilamide removal.

Agricultural Waste Adsorbent	Methods/Technique	Adsorption Capacity (mg/g)	Mechanism	Remarks	Ref.
Carboxyl-functionalized BC derived from walnut shells	Modified with HNO_3	SDZ = 32 SMD = 46 SCF = 40	• Adsorption isotherm: Freundlich model • Kinetic isotherm: Elovich model	The adsorbent has several functional groups that comprise carbon and oxygen, and these functional groups are crucial for sulfonamide adsorption	[58]
Magnetic BC derived from coconut shell	Activation with KOH	SDZ = 294.12 SMT = 400.00 SMX = 454.55	• Adsorption isotherm: Langmuir model • Kinetic isotherm: pseudo-second-order kinetic model	Three successive adsorption–desorption cycles resulted in the retention of more than 80% of the adsorption capacity	[65]
Attapulgite-doped BC derived from rice husk (ATP/BC)		Removal degrees of sulfadiazine and sulfamethazine = 98.63% and 98.24%, respectively	• Adsorption isotherm: Freundlich isothermal model • Kinetic isotherm: pseudo-second-order model (R_2 = 0.99) • Electrostatic interactions, hydrogen bond, π–π interactions, and Lewis acid–base interactions	Sulfonamide adsorption by ATP/BC is a stochastic, heat-absorbing process	[64]
Activated carbon derived from cottonseed husk (CSH-AC)	Pre-treatment of CSH: *Pleurotus ostreatus* was grown on cottonseed husk for 0, 40, and 80 days at 120 °C; followed by NaOH activation	146.16	• Adsorption isotherm: Freundlich model • Adsorption kinetic: pseudo-first-order	The biomass was pre-treated with fungi, which created the desirable physiochemical characteristics for adsorption (well-characterized pore structure, enough surface oxygen-containing functional groups, and suitable hydrophilicity)	[59]
BC derived from sugarcane bagasse	Prepared by hydrothermal carbonization (HTC) followed by NaOH activation	400	• Adsorption isotherm: Freundlich model • Kinetic isotherm: Elovich model • Pore filling followed by charge assisted hydrogen bonding and π-π interaction	Graphitic structure that has been aromatized and aggregated with functional groups that are oxygenated is what causes SMX to be eliminated	[60]
Activated carbon derived from olive pomace (OPAC)		66.22	• Adsorption isotherm: Langmuir model • Adsorption kinetic: pseudo-second-order • π-π electron donor–acceptor	The desorption analysis showed that utilizing ethanol as a solvent achieved the highest desorption ratio of 8.96%	[62]

3. The Adsorption of Non-Steroidal Anti-Inflammatory Medications

3.1. Diclofenac

Diclofenac is a NSAID frequently prescribed to humans and animals to treat inflammation and pain [66]. According to bibliographic data, diclofenac and ibuprofen are Europe's most extensively used NSAIDs [67]. The ecological toxicity of analgesics and anti-inflammatory medications like diclofenac and the elimination capability of traditional wastewater treatment facilities are both concerning. Because these drugs degrade poorly in chemical–biological processes, they are hardly eliminated by conventional wastewater treatment, and the metabolites are transmitted to the aquatic environment [68]. Diclofenac has been found in wastewater and surface water in amounts of up to 2 g/L, and its long-term implications must be investigated [69].

Amongst advanced remediation technologies for these pharmaceutical wastes, the adsorption process typically has high removal efficacy, easiness to operate at a lower cost, and does not produce toxic byproducts. Instead of utilizing the less cost-effective adsorbents such as graphene and AC to remediate water containing diclofenac, adsorbents derived from waste or byproducts in agribusiness and food processing have stood out recently. It includes argan nutshell [69], sunflower seed shell [70], Moringa Oleifera pods [71], orange peel [67], tea waste [72], fique bagasse [66], sycamore ball [73], soybean hull [68], *Melia azedarach* fruit waste [74] and *Cuminum cyminum* agri-waste (CCW) [75]. For example, diclofenac sodium removal in aqueous solution was demonstrated by using tetradecyltrimethylammonium bromide (TTAB) customized CCW [75]. According to the Langmuir isotherm, the maximum adsorption capacity of diclofenac is 93.65 mg/g and the greatest agreement with kinetic behavior of a pseudo-second-order model with R^2 = 0.9981.

Different activating agents affected the adsorption efficiency of diclofenac onto the agricultural waste-derived adsorbents. Phosphoric acid, H_3PO_4, has been proven to be a better activation agent compared to NaOH and KOH, as demonstrated by the higher adsorption capacity of sunflower seed shell [70] and orange peel [67] treated by this acid. It is influenced by several surface functional groups on the surface, including -P_2O_7 and -COOH, and elevated porosity and acidity [70]. On the other hand, the activation of tea waste-derived adsorbent using zinc chloride, $ZnCl_2$, exhibited higher adsorption capacity than other activating agents, including sulfuric acid (H_2SO_4), KOH, and potassium carbonate (K_2CO_3) [72]. However, adsorbent activated by $ZnCl_2$ possess a lower adsorption capacity compared to commercial AC, 62 versus 91 mg/g.

Among other processing parameters, for example temperature, initial concentration of pollutant, and adsorbent dose, the pH of reaction is a pronounced element determining the adsorption efficacy of diclofenac. For example, de Souza, Quesada, Cusioli, Fagundes-Klen, and Bergamasco [68] reported that pH increment from 5 to 10 led to a slight decline in adsorption capacity owing to drug ionization state and functional group dissociation on the adsorbent surface as the pH changed. A similar observation was reported by Viotti, Moreira, dos Santos, Bergamasco, Vieira, and Vieira [71]. An acidic condition of pH 2 is considered optimum for adsorption capacity of diclofenac using orange peel [67]. On the other hand, ionic strength directly influenced system performance, where the suspended salt ions worked as co-adsorbents, promoting adsorption.

Based on isotherm studies, the Langmuir model is commonly favored by the adsorption process of diclofenac, implying the homogeneous monolayer adsorption with uniform free energy change [73]. On contrary, the Freundlich model was the most accurate to represent the adsorption of diclofenac by the adsorbent derived from *Moringa oleifera* pods [71]. Rapid adsorption of diclofenac was observed from the kinetic study. Adsorption capacity of 17.27 mg/g by soybean hull attained equilibrium after 180 min [68], whereas adsorbent derived from argan fruit shell required 60 min to achieve equilibrium [69]. Based on the thermodynamic parameters, adsorption of diclofenac was generally an exothermic process with chemosorption characteristics [71], which involved various interactions, such as electrostatic attractions, Van der Waals forces, π-π stacking and hydrogen-bond formation between the adsorbent and adsorbate [69].

Pyrolysis temperature achieved was 850 and 700 °C in BC (i.e., alternative adsorbent for diclofenac) derived from fique bagasse [66] and *Melia azedarach* fruit [74], respectively. The establishment of aromatic sheets/clusters (i.e., impact to π–π electron donor–acceptor interlinkage between BC and diclofenac) in fique bagasse BC was driven by increased pyrolysis temperature [66]. BC derived from fique bagasse has a lower amount of carbon and higher oxygen content than the other BC, due to its more porous structure it permitted optimal pore filling for diclofenac and thus contributed to the largest adsorption capacities. Table 6 summarizes the adsorption process of diclofenac by the agricultural waste-derived adsorbents and their performance.

Table 6. Agricultural waste-derived adsorbents for removal of diclofenac.

Agricultural Waste	Process Parameters	Kinetics/Isotherm/ Thermodynamics	Maximum Adsorption Capacity (mg/g)	Remarks	Ref.
Cuminum cyminum waste	Adsorbent dose (0.25–6 g/L), contact time (0–300 min), initial diclofenac concentration (10–500 mg/L), and pH	Langmuir/pseudo-second-order	93.65	Both physical and chemical classifications were conducted on the as-prepared adsorbents	[75]
Argan nutshells	Initial concentration (100 mg/L), adsorbent dosage (1 g/L), reaction time (90 min)	Langmuir/pseudo-second-order/spontaneous, exothermic	126	The material stabilized near 600 °C, which explains why this temperature was chosen for carbonization	[69]
Melia azedarach fruit	Adsorbent dosage (50–100 mg), contact time (5–420 min), initial adsorbate concentration (25–200 mg/L), temperature (20–50 °C)	Langmuir, pseudo-second-order, exothermic	5.72	Regeneration experiments for the adsorbates revealed that the biochar has good adsorption efficiency up to three cycles	[74]
Sunflower seed shells (H_3PO_4 activated)	pH (6.5)	Langmuir/pseudo-second-order	690.2	Surface functional groups of $-P_2O_7$, and -COOH developed through H_3PO_4 treatment	
Orange peel	pH (2–6), contact time (5–360 min), initial concentration, temperature (25–35 °C)	Langmuir/pseudo-second-order	122.0	The porous network structure of AC materials is responsible for their surface's rough texture and significant number of cages and cavities	[67]
Sycamore ball	Adsorbent dosage (2.5–30 mg/50 mL), initial concentration (10 to 50 mg/L), temperature (25–45 °C), and pH (2.84–10.20)	Langmuir/pseudo-second-order/exothermic, spontaneous	178.8	Diclofenac's ability to bind to surfaces decreases as adsorption temperature rises due to increased Brownian motion at higher temperatures	[73]
Fique bagasse BC	pH, adsorption time, temperature, initial concentration	Redlich–Peterson/pseudo-second-order	5.40	The volatiles are allowed to escape from the char during the three-hour residence period, which increases the char's porosity and surface area	[66]
Moringa oleifera pods	n/a	Freundlich/pseudo-second-order/endothermic, spontaneous	60.805	Microporous structure and great specific surface area are crucial for the adsorption process	[71]

Table 6. *Cont.*

Agricultural Waste	Process Parameters	Kinetics/Isotherm/ Thermodynamics	Maximum Adsorption Capacity (mg/g)	Remarks	Ref.
Tea waste	Initial concentration (30 mg/L), adsorbent dose (300 mg/L), initial pH (6.47)	Langmuir/pseudo-second-order/endothermic, spontaneous	62	The adsorption process's low activation energy indicate the process is temperature independent	[72]
Soybean hulls	n/a	Sips model/exothermic, spontaneous	96.88	Weakening of the fiber was influenced by the effects of acid, thus explaining the difference in the degradation temperature	[68]

n/a: not applicable.

3.2. Ibuprofen

Ibuprofen is another class of NSAID commonly prescribed for treating mild to moderate pain, infection, fever [67]. The low biodegradability and hydrophilic nature of ibuprofen limits its removal efficiency by conventional water treatment processes [76]. As a result, it has been identified as one of 16 compounds observed in surface, drinking, municipal, and groundwater from all United Nations five regional groups, with worldwide average values ranging from 0.032 to 0.922 g/L [77]. They tend to bioaccumulate due to their resistance to natural breakdown via mechanisms such as light and heat, causing toxicity to aquatic biota [78]. Thus, eliminating it from water bodies is crucial. According to Costa, do Nascimento, de Araújo, Vieira, da Silva, de Carvalho, and de Faria [78], carbon-based adsorbents are the best type of adsorbent for the remediation of ibuprofen. Studies have been conducted to study the ability of agricultural waste-derived adsorbents for the elimination of ibuprofen in water. It includes the utilization of sunflower seed shell [70], coconut shell [79], *Moringa stenopetala* seeds [80], orange peel [67], murumuru waste [78], spent coffee waste [76], and *Erythrina speciosa* pods [81].

The removal percentage of ibuprofen onto the *Erythrina speciosa* pods AC is directly proportional to the adsorbent dosage amount on the increment of the active binding sites on the adsorbent to retain the ibuprofen molecules [81]. The greater the pH of the reaction solution, the more negative charge accumulated on the adsorbent surface, reducing adsorption capacity due to ibuprofen repelling. In addition to pH, the adsorption capacity and affinity of adsorbents for ibuprofen elimination are both controlled by the occurrence of numerous contaminants and the ionic strength of the solution [76]. NaOH-activated spent coffee wastes showed viable adsorption of pharmaceuticals products on the BC occurred more freely over the entire ionic strength in the NaCl range 0–0.125 M [76]. According to Matějová, Bednárek, Tokarský, Koutník, Sokolová, and Cruz [77], the micropore volume and size together with the fast rate of graphitization governed the adsorption capacity of AC on ibuprofen [77]. They bond predominantly via electrostatic and hydrophobic interactions, weak hydrogen bonds, π-π stacking, and dipole-interactions [82]. Adsorption capacity of BC from sunflower seed shells treated using H_3PO_3 was higher compared to NaOH due to numerous surface functional groups (e.g., -P_2O_7, and -COOH) along with great porosity and acidity condition [70].

The adsorption of ibuprofen onto the coconut shell-derived AC [79] and *Moringa stenopetala* seeds [80] was proven to obey Langmuir, based on the R^2 value, indicating a monolayer adsorption onto a surface having a limited quantity of same sites. The kinetic behavior of agriculturally derived AC throughout the ibuprofen adsorption was better suited to the pseudo-second-order model, implying that adsorption is caused by relations between the aromatic and oxygenated groups existing on the adsorbent's surface and in the adsorbate's molecular structure [78]. Adsorption of ibuprofen was reported to be influenced by both their initial concentration and the amount of pores on the adsorbent [82].

The positive value of ΔH^0 designates that the ibuprofen adsorption process is endothermic and physical in nature [67], while positive ΔS^0 value revealed that the system disruption at the interface decreased during adsorption [81]. Table 7 summarizes the adsorption process of ibuprofen utilizing agricultural waste-derived adsorbents.

Table 7. Agricultural waste-derived adsorbents for removal of ibuprofen.

Agricultural Waste	Process Parameters	Kinetics/Isotherm/ Thermodynamics	Maximum Adsorption Capacity (mg/g)	Remarks	Ref.
Sunflower seed shells (H_3PO_4 activated)	pH (6.5)	Langmuir isotherm, pseudo-second-order kinetics	105.7	Activated agents such as H_3PO_4 and NaOH used to synthesis the biochar	[70]
Coconut shell	Initial concentration (200–1000 mg/L), contact time (10–200 min), temperature (30–60 °C)	Langmuir isotherm, pseudo-first-order, endothermic and non-spontaneous thermodynamics	63.78	All of the functional groups found on the adsorbents surface had a significant impact on the way that ibuprofen solutions behaved.	[79]
Moringa stenopetala seed protein	Adsorbent dosage (50–100 mg), contact time (5–420 min), initial adsorbate concentration (25–200 mg/L), temperature (20–50 °C)	Langmuir	n/a	pH plays the most important role in maximizing the adsorption capacity compared to other parameters	[80]
Orange peel	pH (2–6), contact time (5–360 min), initial concentration, temperature (25–35 °C)	Langmuir isotherm, pseudo-second-order kinetics, endothermic and spontaneous thermodynamics	66	Low removal capacity of ibuprofen is due to the presence of only one carboxyl group	[67]
Waste murumuru (*Astrocaryum murumuru* Mart)	Adsorbent dosage (0.15 g), pH (3.0), adsorption time (360 min)	Freundlich isotherm, pseudo-second-order kinetics, endothermic, physical, and spontaneous thermodynamics	>2.2	Ibuprofen adsorption was through physisorption; ΔG° between 0 and −20 KJ/mol	[78]
Spent coffee waste	pH (5.0–11.0), ionic strength (NaCl: 0–0.125 M)	Spontaneous	61.25–80.02 (μmol/g)	Chemisorption plays an important role in this adsorbent	[76]
Erythrina speciosa pods	pH (3–9), adsorbent dosage (0.4–1.2 g/L)	Langmuir isotherm, linear driving force (LDF) kinetics, spontaneous, favorable, and endothermic thermodynamics	98.11	The same excellent adsorption capacity was observed for use up to 7 times	[81]

n/a: not applicable.

3.3. Aspirin

Aspirin (acetyl salicylic acid) is one of the most common over-the-counter painkillers used to relieve pain and inflammation, and to prevent heart attacks, angina, and strokes [83]. The World Health Organization's (WHO) List of Essential Medicines listed aspirin, with

around 35,000 tons of aspirin consumed worldwide, each year. Aspirin has been identified as an emergent pollutant in aquatic habitats as a result of its widespread manufacture and use, with amounts varying from nanograms to micrograms per liter being observed [84]. The severity of the risk of aspirin-containing wastewater has raised concerns about resolving this issue since it is capable of causing fatality to microorganisms, particularly through its chronic effects, despite its low concentration in wastewater.

Recently, several studies have reported using agricultural waste-based adsorbents as a more cost-effective option for removing aspirin from water. Such approaches included utilization of *Zizyphus mauritiana* seeds and *Balanites aegyptiaca* seeds [85], laccase-immobilized date stone [86], spent tea leaves [9,87], orange peel [67], sugarcane bagasse [88], and rice husk [89]. Chemical or heat treatment of agricultural waste-derived adsorbent significantly improved their performance against pharmaceutical pollutants including aspirin. For example, chemical treatments of date stones using sulfuric acid, H_2SO_4, increased their surface area by 36-fold, making carbonyl groups become more pronounced [86]. The existence of functional groups (e.g., carboxyl and hydroxyl) on thermally treated (105 °C, 2 h) rice husk may be the primary sorption sites for aspirin elimination that further enhances the adsorption capacity of the rice husk [89]. Low surface energy (K_L value less than 0.1) demonstrated by adsorbents made by *Zizyphus mauritiana* and *Balanites aegyptiaca* seeds is an sign of robust bonding between aspirin and the adsorbents [85]. Orange peel treated by H_3PO_4 at 650 °C gave a porous structure to a network that contributed to a rougher surface morphology, characterized by a large number of cages and holes [67].

For the thermodynamics study, Malesic-Eleftheriadou, Liakos, Evgenidou, Kyzas, Bikiaris, and Lambropoulou [67] revealed that adsorption is favored at elevated temperatures, as shown by the negative entropy, ΔG_o values at the elevated temperature, and positive ΔH_o values, which indicated that adsorption presents an endothermic nature. Moreover, the spent tea leaf activated via microwave irradiation was revealed to have two times higher Brunauer–Emmett–Teller (BET) surface area and total pore volume with 51% mesopore volume representing the high mesoporosity of the adsorbent [87]. Pyrolytic degradation of waste tea leaves manufactured using H_3PO_4 have higher textural qualities and presence of a cross-link network between the phosphate and fragments in biomass [87]. The Liu isotherm model represents the adsorption equilibrium for BC, implying that the carbonized surface is heterogeneous in character, with high adsorption effectiveness at low pH [88].

The Langmuir isothermal model shows a slightly good fit to the process. It indicates the formation of a uniform monolayer of aspirin onto the adsorbent used, including activated date stone [86], rick husk AC [89], *Zizyphus mauritiana* and *Balanites aegyptiaca* seeds [85]. Chemisorption was the rate-deciding step in the adsorption process of aspirin, as demonstrated by the correlation coefficient for the pseudo-second-order kinetic model [86]. Table 8 summarizes the adsorption of aspirin utilizing agricultural waste-derived adsorbents.

Table 8. Agricultural waste-derived adsorbent for removal of aspirin.

Agricultural Waste	Process Parameters	Kinetics/Isotherm/ Thermodynamics	Maximum Adsorption Capacity (mg/g)	Remarks	Ref.
Laccase-immobilized date stone	pH (2–7), temperature (10–60 °C), ABTS (0.1–0.6), storage time (0–30 days)	Langmuir isotherm, pseudo-second-order kinetic, endothermic	458.71	The removal process was both conducted by enzymatic activity and adsorption	[86]

Table 8. *Cont.*

Agricultural Waste	Process Parameters	Kinetics/Isotherm/ Thermodynamics	Maximum Adsorption Capacity (mg/g)	Remarks	Ref.
Spent tea leaves	Initial concentration (100 mg/L), adsorbent dosage (0.5 g), pH (3), temperature (30 °C), reaction time (60 min)	Freundlich isotherm, pseudo-second-order kinetics, exothermic and spontaneous thermodynamics	178.57	H_3PO_4 is the best agent to utilize in the chemical activation of STL-AC, as indicated by 68.04% of adsorption performance	[87]
Orange peel	pH (2–6), contact time (5–360 min), initial concentration, temperature (25–35 °C)	Langmuir isotherm, pseudo-second-order kinetics, endothermic and spontaneous thermodynamics	47	The ideal pH for the adsorption was 2, and the pseudo-second-order kinetic rule suggests that the entire adsorption process can be completed in 3 h	[67]
Sugarcane bagasse BC	pH, temperature, and time	Liu isotherm model, pseudo-second-order	32.73	C- and O-containing functional groups of the adsorbents are responsible in the adsorption process	[88]
Rice husk	pH (2)	Langmuir	47.03	Acidic surface of adsorbents is validated by pH_{pzc} 5.8 and pH 2 is the best pH	[89]
Zizyphus mauritiana seeds	Reaction time (180 min), adsorbent dosage (0.5 g), initial concentrations (0 to 100 mg/L)	Langmuir	8.95	Existence of monolayer adsorption of aspirin	[85]
Balanites aegyptiaca seeds	Reaction time (180 min), adsorbent dosage (0.5 g), initial concentrations (0 to 100 mg/L)	Langmuir	7.40	Existence of monolayer adsorption of aspirin	[85]

3.4. Ketoprofen

Ketoprofen is one NSAID that is extensively prescribed to the humans, especially elderly, to cure osteoarthritis, spondylitis, rheumatoid arthritis, and various kinds of pain [67]. Despite its efficacy in alleviating pain, the availability of a huge quantity of the drug and its widespread utilization has resulted in the occurrence of the drug in wastewater treatment facilities and rivers, with a concentration ranging from 3.15 ng/L to 209 µg/L [90]. Ketoprofen was detected in drinking water in Algeria at concentrations of up to 273 ng/L, while it is one of the most commonly found pharmaceuticals in Taiwanese rivers with concentrations extending from 110 to 620 ng/L [91]. Its residual concentration is greater in regions with elderly populations [92]. Due to the ecotoxicity risk that posed by this pollutant and the inefficiency of the current wastewater treatment facilities to mitigate this issue, suitable remediation technologies must be proposed. In response, studies have been conducted to discover the capability of inexpensive adsorbents derived from agricultural waste, including *Fagopyrum esculentum* wheat husks [93], coconut shell [79], *Moringa stenopetala* seeds [80], orange peel [67], *Jacaranda mimosifolia* seed pods [94], *Physalis peruviana* fruit residue [95], *Campomanesia guazumifolia* bark [96], *Dillenia indica* peel [97], and laccase-immobilized date stone [86].

The adsorption capacity of the pharmaceutical waste including ketoprofen was directly proportional to the pH, pKa, and pH point of zero charge [92]. Georgin, Yamil, Franco, Netto, Piccilli, Perondi, Silva, Foletto, and Dotto [94] demonstrated that the material (i.e., highly porous AC from *Jacaranda mimosifolia*) achieved pH at the point of zero charge of

4.1 with the best adsorption at pH 2. The isotherm study discovered that the adsorption capacity declined with temperature and followed the Langmuir model. Synergistic effects between date stones as adsorbent and immobilized laccase responsible for enzymatic degradation nearly reached complete removal of ketoprofen, best fit by using the Freundlich isotherm model compared to the Langmuir isotherm model [86]. An extreme reduction in ketoprofen removal efficiency by 42.7% was observed when the pH was increased from 7 to 9 [80]. This is due to a decrease in the intensity of the positive charge on the water-soluble protein molecules at pH > 6. This acidic condition was favorable in other adsorption studies as well, where the maximum adsorption capacity was achieved at pH (2) [96] and pH 6 [97]. Multi-layer adsorption was profoundly influenced by the solution temperature, wherein a multi-molecular process was predictable for a ketoprofen adsorption system, as demonstrated by *Physalis peruviana* biomass, by which each binding site of this biomass may adsorb multiple molecules simultaneously ($n_m > 1$) [95].

However, an opposite trend was observed by Malesic-Eleftheriadou, Liakos, Evgenidou, Kyzas, Bikiaris, and Lambropoulou [67], where the increment of temperature from 25 to 35 °C was found to have a constructive effect on the adsorption capacity, which also depends on the assortment of functional groups within chemical structures of NSAIDs. This includes ketoprofen that has one carboxylic group and one keto group. Physical models are governed in a study on adsorption of ketoprofen using wheat husks *Fagopyrum esculentum* to identify several data including the number of adsorbate layers [93]. Heterogeneous formation of adsorbate layers (five to six layers) occurred, while a rise in temperature can cause a profound inactivation of some adsorption sites, thus reducing adsorption capacity and the total number of generated layers. Table 9 summarizes the process parameters and mechanism conditions for the adsorption of ketoprofen by agricultural waste-derived adsorbents.

Table 9. Agricultural waste-derived adsorbents for removal of ketoprofen.

Agricultural Waste	Process Parameters	Kinetics/Isotherm/ Thermodynamics	Maximum Adsorption Capacity (mg/g)	Remarks	Ref.
Physalis peruviana fruit residue	n/a	Endothermic	172	The removal of adsorbate using physical adsorption forces (adsorption energies less than 40 kJ/mol)	[95]
Fagopyrum esculentum wheat husks	Adsorbent dosage (0.5–1.5 g L^{-1}), pH (2–10)	Exothermic	n/a	Greater irregularities and new spaces appeared after treatment with H_2SO_4, crucial in the adsorption process	[93]
Coconut shell	Initial concentration (200–1000 mg/L), contact time (10–200 min), temperature (30–60 °C)	Temkin/pseudo-first-order/endothermic, non-spontaneous	73.78	Adsorptive capacity increased with concentration up to 150 min	[79]
Moringa stenopetala seeds	Adsorbent dosage (50–100 mg), contact time (5–420 min), initial adsorbate concentration (25–200 mg/L), temperature (20–50 °C)	Langmuir	n/a	Sudden drop of removal efficiency when pH increased from 7 to 9	[80]
Orange peel	pH (2–6), contact time (5–360 min), initial concentration, temperature (25–35 °C)	Langmuir/pseudo-second-order/endothermic, spontaneous	78	Functional groups of ketoprofen (one keto group and one carboxylic group) crucial in high adsorption percentage	[67]

Table 9. *Cont.*

Agricultural Waste	Process Parameters	Kinetics/Isotherm/ Thermodynamics	Maximum Adsorption Capacity (mg/g)	Remarks	Ref.
Jacaranda mimosifolia seed pods	pH (2–10), adsorbent dosage (0.5–1.5 g/L), initial concentration (100, 150, and 200 mg/L), contact time (0–240 min)	Langmuir/linear driving force/spontaneous, exothermic	303.9	The KET adsorption is favored by a rough surface with granular and heterogeneous particles, newly formed pores with irregularly sized, randomly distributed pores	[94]
Campomanesia guazumifolia bark	Initial concentration (50, 75, and 100 mg/L), pH (2), temperature (298, 308, 318, 328 K), contact time (6 h)	Langmuir/Elovich kinetics/exothermic	158.3	Extension of the carbonyl group present in hemicellulose and new textural shape formed with new pores and cavities after acid treatment	[96]
Dillenia Indica peel	Adsorbent dosage (0.2–1.0 g), initial concentration (20–100 mg/L), pH (2–12)	Langmuir/pseudo-second-order	8.354	Adsorption is favorable at lower pH	[97]
Laccase-immobilized date stone	pH (2–7), temperature (10–60 °C), ABTS (0.1–0.6), storage time (0–30 days)	Pseudo-second-order/Freundlich model/endothermic	568.18	Synergistic effect of both enzymatic degradation and adsorption take place in ketoprofen removal	[86]

n/a: not applicable.

3.5. Naproxen

Naproxen is a class of medicine with anti-inflammatory, pain-killer, and anti-pyretic action. It functions by lowering the body's synthesis of chemicals that cause pain or fever [98]. These drugs do not adsorb completely in the body and hence eliminated via urination. They move to the water bodies and may not be effectively removed by conventional wastewater treatment [98]. These drugs are found in surface water, wastewater, groundwater, and drinking water worldwide, at up to 2.3 mg/L, and listed on the Global Water Research Coalition (GWRC) priority list [99]. Adsorption is a prominent approach for treating naproxen-containing wastewater owing to its simplicity and easy operation [100].

Various materials were studied as adsorbents for potentially eliminating this pollutant in aqueous solutions, for example, coconut shell [79], grape tree fruit peel [100], grape branches [101], *Dillenia indica* peels [102], wild plum kernels [99], and pitaya and jabuticaba peel [98]. An activation step for the biosorbent precursor improved their morphology, hence increasing their adsorptive performance towards naproxen. The diffusion of metallic potassium into the internal structure of the lignocellulosic material during the microwave-assisted activation of wild plum kernel by KOH produced micropores and a range of surface functionalities, mainly oxygen-containing groups, on the BC [99].

Spent coffee waste activated with NaOH has shown a better adsorption capacity towards naproxen than the pristine phase, substantially improved through its physicochemical properties (higher specific surface area, total pore volume, and aromaticity) [76]. Naproxen is an acidic pharmaceutical with a pKa of 4.2; thus, at pH levels greater than pKa, it is mostly in its anionic form in solution owing to deprotonation [99]. The electrostatic repulsion that arises between the charges in the adsorbate and the adsorbent caused a drop in the adsorption capacity of the adsorbent towards naproxen as the pH increased from 3 to 10 [78]. The acidic and hydrophilic activity may occur due to the hydrogen within the carboxylic group, which is ionizable at pH higher than its pK_a value [99].

Furthermore, with increasing adsorbent mass, concomitant declines in adsorption capabilities were found because of rising diffusive resistance and decreased effective surface area produced by overlapping adsorption sites. The maximum adsorption capacity

of the AC derived from grapetree fruit peels and grape branches showed high surface area, 1033 m^2 g^{-1} [100] and 938 m^2 g^{-1} [101], respectively; this is the most crucial element to adsorb naproxen from the effluents. The Langmuir and Temkin isotherm models and pseudo-second-order model in the kinetic analysis for *Dillenia indica* peel adsorption data were mentioned and the chemisorption mechanism regulated the adsorption that ensues as a monolayer [102]. Based on the thermodynamics study by Franco, Georgin, Netto, da Boit Martinello, and Silva [98], naproxen adsorption is via physical mechanisms, relying on hydrogen bonds, electrostatic differences, and possibly π-π interaction. The FTIR data presented by Paunovic, Pap, Maletic, Taggart, Boskovic, and Sekulic [99] also demonstrated that hydrogen bonding and π-π and n-π electron donor–acceptor interactions also contributed to naproxen removal. Table 10 summarizes the agricultural waste-derived adsorbents for removal of naproxen. Figure 4 shows the summary of agricultural waste used as adsorbents for NSAIDs wastewater treatment.

Table 10. Agricultural waste-derived adsorbents for removal of naproxen.

Agricultural Waste	Process Parameters	Kinetics/Isotherm/ Thermodynamics	Maximum Adsorption Capacity (mg/g)	Remarks	Ref.
Grapetree fruit peel	pH (2–10), temperature (298–328 K), initial concentration (0–125 mg/L)	Langmuir isotherm, linear driving force model, spontaneous and endothermic thermodynamics	167.03	Increased carbon content (85.6%) and decreased oxygen content (below 10%) of adsorbent is evidence for a significant loss of volatile matter	[100]
Coconut shell	Initial concentration (200–1000 mg/L), contact time (10–200 min), temperature (30–60 °C)	Pseudo-first-order, Freundlich isotherm, endothermic, non-spontaneous	73.78	The adsorptive capacity of adsorbent was increased with concentration up to 150 min	[79]
Grape branches (*Vitis vinifera*)	Temperature (298–328 K), initial concentration (0–50 mg/L)	Linear driving force model, Langmuir, endothermic and spontaneous	176	With an HCl solution, the adsorbent can be regenerate up to seven times	[101]
Dillenia indica peels	Adsorbent dosage (0.2–1), contact time (0–500 min), pH (2–12), and initial drug concentrations (20–100 mg/L)	Langmuir and Temkin isotherm, pseudo-second-order kinetics	10.76	The best parameter of adsorption was pH 5.0, adsorbent dosage 0.4 g, contact time 480 min	[102]
NaOH-activated spent coffee waste	Initial concentration (10–50 mM), agitation time (0–24 h), pH (5–11), temperature (15–35 °C), ionic strength (NaCl: 0–0.125 M)	Langmuir, pseudo-second-order kinetics, endothermic	263.34 (wastewater), 269.01 (lakewater)	NaOH-activated SCW biochar adsorption capacity is closely associated with π-π interaction between the adsorbates and the carbonaceous adsorbents	[76]
Wild plum kernel	pH (2–11), adsorbent dosage (2–200 mg), contact time (5–420 min), initial concentration (3.1–125.3 mg/L)	Langmuir, pseudo-second-order kinetics	73.14	The diffusion rate constants, Ki, rose from 0.469 to 1.264 mg/g min1/2 with increased initial concentration whereas C values declined, indicating that diffusion was quicker at greater concentrations	[99]

Table 10. *Cont.*

Agricultural Waste	Process Parameters	Kinetics/Isotherm/ Thermodynamics	Maximum Adsorption Capacity (mg/g)	Remarks	Ref.
Pitaya (*Hylocereus undatus*) peels	Temperature (298, 308, 318, and 328 K), initial concentration (10, 20, 30, 40, 50 mg/L)	Spontaneous, exothermic	158.81	Given that the evolution of temperature only affects one site's density of naproxen adsorption, temperature has a small impact	[98]
Jabuticaba fruit peels	Temperature (298, 308, 318, and 328 K), initial concentration (50, 85, 100, and 125 mg/L)	Spontaneous, exothermic	167.0	Density of the first and second sites leads to naproxen adsorption increasing with the evolution in temperature	[98]
Grapefruit branches	Temperature (298, 308, 318, and 328 K), initial concentration (10, 20, 30, 40, 50 mg/L)	Spontaneous, exothermic	176.0	Quantity of naproxen molecules decreases with evolution in the system's temperature	[98]
Waste of *Astrocaryum murumuru* Mart.	Adsorbent dosage, contact time, and pH	Pseudo-second-order/Freundlich/ endothermic, physical, spontaneous	2.5	Adsorbent with low S_{BET} and well-developed microporosity	[78]

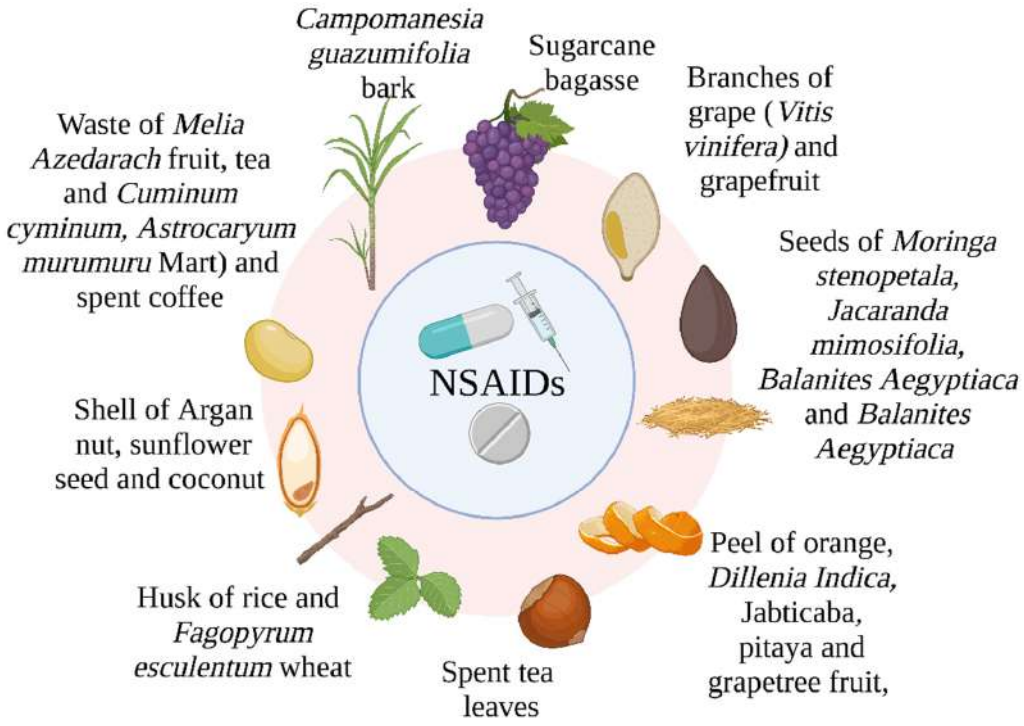

Figure 4. Summary of agricultural waste used as adsorbents for NSAIDs wastewater treatment.

4. Adsorption Mechanism for Antibiotics and NSAIDs

Physical and chemical adsorption may be used to summarize the nature of adsorption and its mechanism, as demonstrated below (Figure 5). The key functions of the physisorption or physical adsorption process are the weak van der Waals interactions, pore filling/size-selective adsorption, and π-π interactions since the mechanism is entirely reliant on the nature of the adsorbate and adsorbent. Contrarily, the mechanism of chemical adsorption or chemisorption involves the development of inner-sphere coordination complexes or surface chemical bonds on the surfaces of the adsorbent and adsorbate through

electron transfer via ion/ligand exchange, Lewis acid–base interaction, and oxidation or reduction [103].

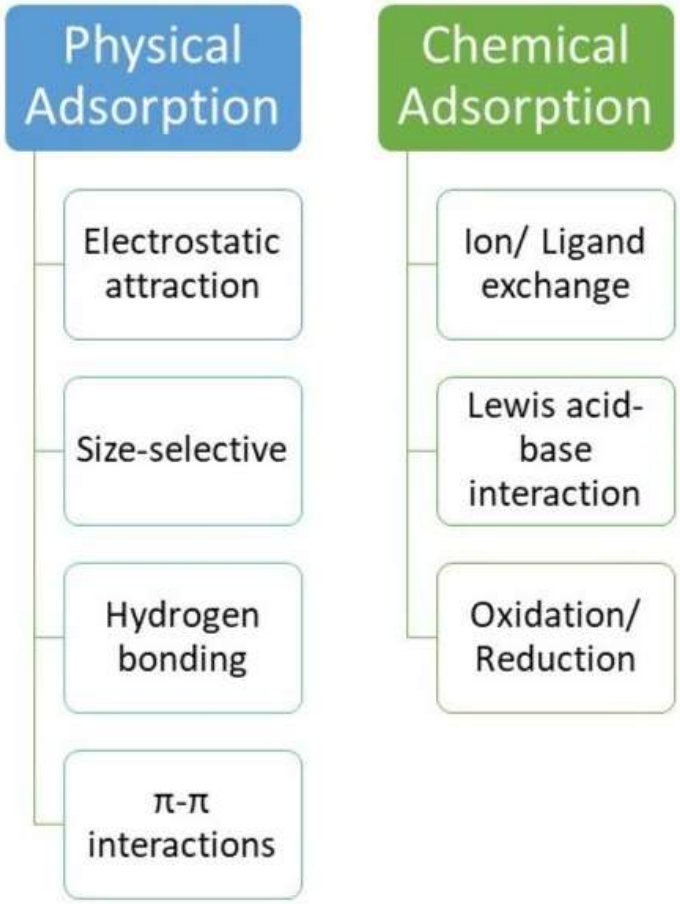

Figure 5. Classification of physical and chemical adsorption mechanisms.

Reliant on the pH of the solution, antibiotics and NSAIDs may remain in the environment as ionized compounds with positive or negative charges. Antibiotics and NSAIDs with adsorbents may exhibit electrostatic attraction and repulsion between their cationic and anionic forms under acidic and alkaline environments. By adjusting the ionic strength of the aqueous medium, electrostatic interactions may be made more or less attractive or repulsive. Moreover, conjugated benzene rings, pyrrole rings, and other groups with -electron density are present in antibiotics and NSAIDs and other compounds. The concept of -electron donor–acceptor interaction has been acknowledged as an efficient adsorption mechanism [104]. The benzene ring and the unshared pair of e act in strong e interaction, and both are able to form strong networks with positively charged sites on adsorbents for agricultural waste. Furthermore, NSAIDs and antibiotics that include functional groups such as -OH, -NO_2, and -COOH may create H-bonds with the adsorbent surface. According to Patel et al. [105], hydrogen bond formation between antibiotic molecules and carbonyl groups of banana peel biochar played a significant part in the adsorption process. Additionally, a previous study reported the elimination of antibiotics through dipole interactions [106]. For example, in a recent study by Liu et al. [107], the authors highlighted that the oxygen-containing functional groups on the corn stover-based adsorbent surface, such as COOH, OH, and ether groups, could interact with carbonyl and hydroxyl groups of the naproxen via dipole–dipole interaction. Based on the abovementioned studies on the removal of antibiotics and NSAIDs using adsorbents from agricultural waste, the adsorption mechanism of antibiotics and NSAIDs is summarized in Figures 6 and 7, respectively.

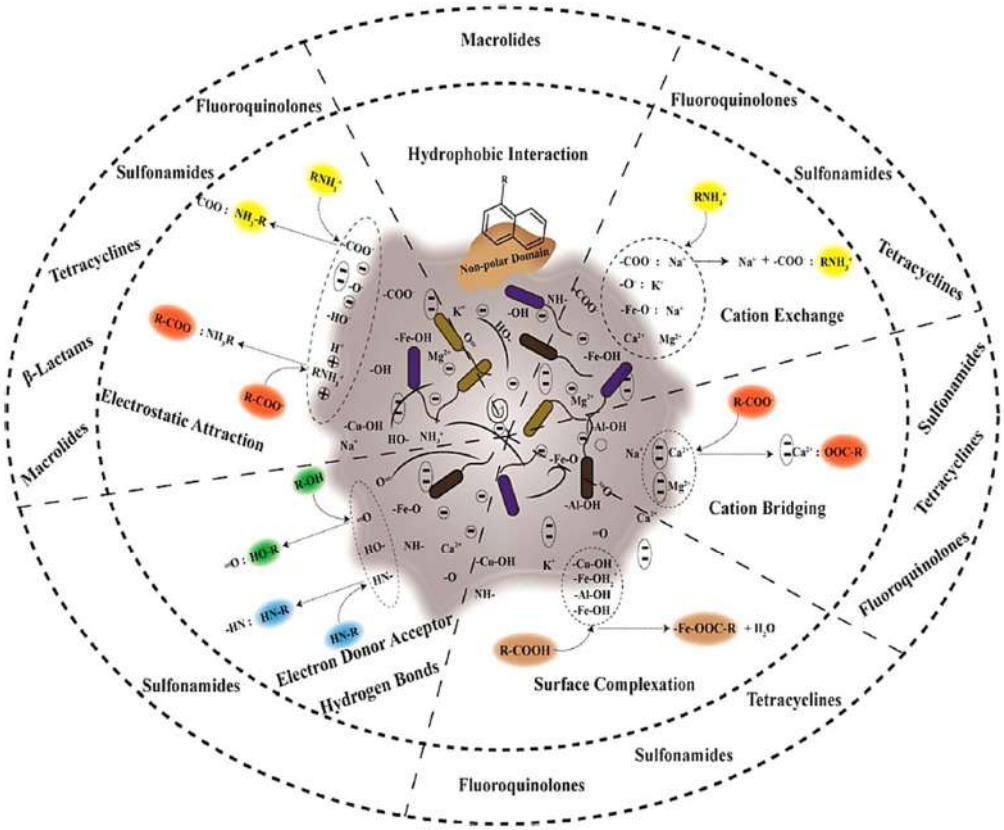

Figure 6. Summary of antibiotic adsorption mechanisms by agricultural waste adsorbents [108].

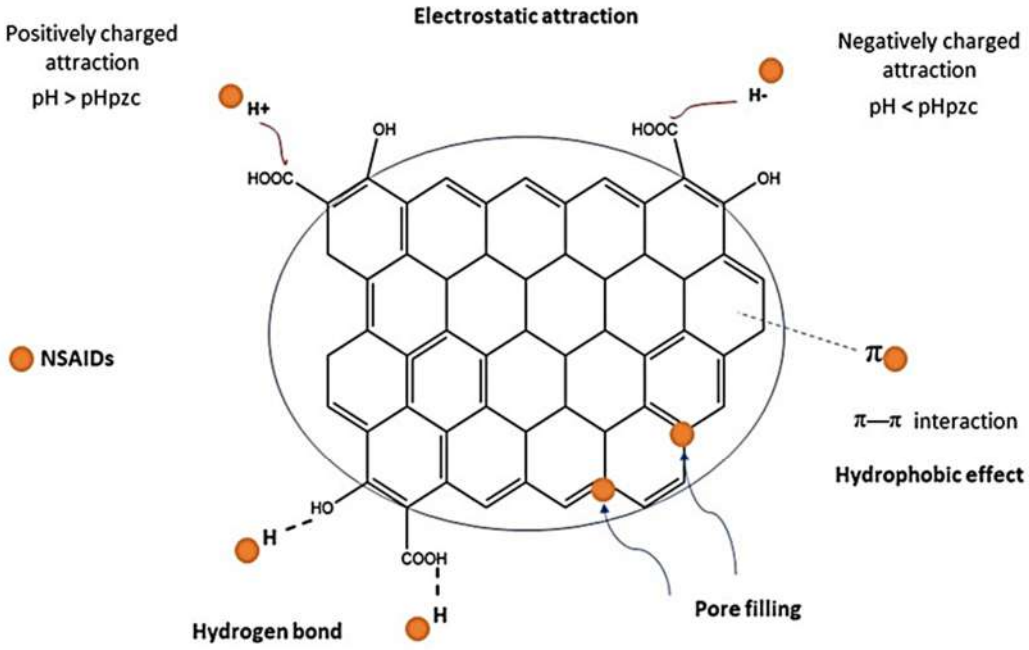

Figure 7. Summary of NSAIDs adsorption mechanisms by agricultural waste adsorbents.

5. Limitation and Future Perspective

There has been substantial investigation on the effectiveness of agricultural waste as an adsorbent for the adsorption of antibiotics and NSAIDs. The viability of employing such materials is only assessed on a small-scale in laboratories, despite the enormous number of studies that have been reported. Moreover, waste products from agriculture are not known

to be stable. It is impossible to use the removal efficiency as a stability indicator. The usage of these materials may be restricted by a decrease in removal effectiveness in practical wastewater applications. In this regard, the following is suggested for further research on the adsorption of pharmaceutical waste by agricultural waste: Low-cost adsorbents are essential to remove pollutants at pilot and industrial scales. The investigation will be broadened to include examinations of the competitive adsorption of medications with further kinds of contaminants, such as metals and new organics, to highlight the analysis at molecular level of the substance's adsorption-retaining capabilities. Finally, investigation on the actual pharmaceutical wastewater is preferable than simulative prepared wastewater.

6. Conclusions

A variety of agricultural waste products have been discussed in this study for the removal of pharmaceutical pollutants from wastewater. Even though many articles have been published regarding the applications of agricultural waste in wastewater treatment, there is still a dearth of material offering a thorough discussion on the removal of pollutants from the antibiotic and NSAID classes. This review aids readers in comprehending the state of the art in pharmaceutical pollutants adsorption studies, particularly concerning antibiotics (e.g., tetracycline, amoxicillin, norfloxacin, chloramphenicol, and sulfanilamide) and NSAIDs (e.g., diclofenac, ibuprofen, aspirin, ketoprofen, and naproxen) by low-cost adsorbents from agricultural waste sources. Agricultural wastes were utilized as adsorbents because they are simple to gather and prepare, have chemical groups that encourage the adsorption of pollutants, and have a large surface area. The capability of agricultural waste adsorbents to bind antibiotics and NSAIDs is influenced by several parameters, such as the initial pharmaceutical concentration, pH, and dose of the adsorbents. Their adsorption mechanisms cannot be described by a single model. Overall, agricultural waste-based adsorbents have important benefits to presently costly commercial AC for the reduction in water pollution, and they may also help with a comprehensive waste management plan.

Author Contributions: Conceptualization, A.H.N., A.S.N. and S.F.M.N.; validation, A.H.N. and S.M.N.H.; investigation, A.H.N., A.S.N., S.F.M.N. and S.H.P.; writing—original draft preparation, A.H.N., A.S.N. and S.F.M.N.; writing—review and editing, A.H.N., S.H.P., S.M.N.H., M.L.N., R.A.I., N.N., A.A.B., Z.A., M.S.A., W.I.N. and W.N.; funding acquisition, M.L.N. All authors have read and agreed to the published version of the manuscript.

Funding: This work was funded by a Research University grant from Universiti Teknologi Malaysia (Vot no. Q.J130000.3851.18J95).

Data Availability Statement: Not applicable.

Acknowledgments: Abu Hassan Nordin, the first author, would like to extend his sincere appreciation to University Teknologi Malaysia for the financial support given via the Zamalah scholarship program.

Conflicts of Interest: The authors declare no conflict of interest.

References

1. Grela, A.; Kuc, J.; Bajda, T. A review on the application of zeolites and mesoporous silica materials in the removal of non-steroidal anti-inflammatory drugs and antibiotics from water. *Materials* **2021**, *14*, 4994. [CrossRef] [PubMed]
2. Chakhtouna, H.; Benzeid, H.; Zari, N.; Bouhfid, R. Functional $CoFe_2O_4$-modified biochar derived from banana pseudostem as an efficient adsorbent for the removal of amoxicillin from water. *Sep. Purif. Technol.* **2021**, *266*, 118592. [CrossRef]
3. Izadi, P.; Izadi, P.; Salem, R.; Papry, S.A.; Magdouli, S.; Pulicharla, R.; Brar, S.K. Non-steroidal anti-inflammatory drugs in the environment: Where were we and how far we have come? *Environ. Pollut.* **2020**, *267*, 115370. [CrossRef] [PubMed]
4. He, X.; Kai, T.; Ding, P. Heterojunction photocatalysts for degradation of the tetracycline antibiotic: A review. *Environ. Chem. Lett.* **2021**, *19*, 4563–4601. [CrossRef]
5. Feng, L.; Watts, M.J.; Yeh, D.; Esposito, G.; van Hullebusch, E.D. The efficacy of ozone/BAC treatment on non-steroidal anti-inflammatory drug removal from drinking water and surface water. *Ozone Sci. Eng.* **2015**, *37*, 343–356. [CrossRef]
6. da Silva, T.L.; Costa, C.S.D.; da Silva, M.G.C.; Vieira, M.G.A. Overview of non-steroidal anti-inflammatory drugs degradation by advanced oxidation processes. *J. Clean. Prod.* **2022**, *346*, 131226. [CrossRef]

7. Nadais, H.; Li, X.; Alves, N.; Couras, C.; Andersen, H.R.; Angelidaki, I.; Zhang, Y. Bio-electro-Fenton process for the degradation of non-steroidal anti-inflammatory drugs in wastewater. *Chem. Eng. J.* **2018**, *338*, 401–410. [CrossRef]
8. Koltsakidou, A.; Katsiloulis, C.; Evgenidou, E.; Lambropoulou, D. Photolysis and photocatalysis of the non-steroidal anti-inflammatory drug Nimesulide under simulated solar irradiation: Kinetic studies, transformation products and toxicity assessment. *Sci. Total Environ.* **2019**, *689*, 245–257. [CrossRef]
9. Nordin, A.H.; Ngadi, N.; Ilyas, R.A.; Abd Latif, N.A.F.; Nordin, M.L.; Mohd Syukri, M.S.; Nabgan, W.; Paiman, S.H. Green surface functionalization of chitosan with spent tea waste extract for the development of an efficient adsorbent for aspirin removal. *Environ. Sci. Pollut. Res.* **2023**, 1–18. [CrossRef]
10. Zhang, X.; Kamali, M.; Xue, Y.; Li, S.; Costa, M.E.V.; Cabooter, D.; Dewil, R. Periodate activation with copper oxide nanomaterials for the degradation of ciprofloxacin-A new insight into the efficiency and mechanisms. *J. Clean. Prod.* **2023**, *383*, 135412. [CrossRef]
11. Nordin, A.H.; Wong, S.; Ngadi, N.; Zainol, M.M.; Abd Latif, N.A.F.; Nabgan, W. Surface functionalization of cellulose with polyethyleneimine and magnetic nanoparticles for efficient removal of anionic dye in wastewater. *J. Environ. Chem. Eng.* **2021**, *9*, 104639. [CrossRef]
12. Birniwa, A.H.; Abubakar, A.S.; Huq, A.O.; Mahmud, H.N.M.E. Polypyrrole-polyethyleneimine (PPy-PEI) nanocomposite: An effective adsorbent for nickel ion adsorption from aqueous solution. *J. Macromol. Sci. Part A* **2021**, *58*, 206–217. [CrossRef]
13. Foroutan, R.; Mohammadi, R.; Farjadfard, S.; Esmaeili, H.; Saberi, M.; Sahebi, S.; Dobaradaran, S.; Ramavandi, B. Characteristics and performance of Cd, Ni, and Pb bio-adsorption using Callinectes sapidus biomass: Real wastewater treatment. *Environ. Sci. Pollut. Res.* **2019**, *26*, 6336–6347. [CrossRef]
14. Kadhom, M.; Albayati, N.; Alalwan, H.; Al-Furaiji, M. Removal of dyes by agricultural waste. *Sustain. Chem. Pharm.* **2020**, *16*, 100259. [CrossRef]
15. Xue, Y.; Guo, Y.; Zhang, X.; Kamali, M.; Aminabhavi, T.M.; Appels, L.; Dewil, R. Efficient adsorptive removal of ciprofloxacin and carbamazepine using modified pinewood biochar–A kinetic, mechanistic study. *Chem. Eng. J.* **2022**, *450*, 137896. [CrossRef]
16. Salleh, M.A.M.; Mahmoud, D.K.; Karim, W.A.W.A.; Idris, A. Cationic and anionic dye adsorption by agricultural solid wastes: A comprehensive review. *Desalination* **2011**, *280*, 1–13. [CrossRef]
17. Dai, Y.; Sun, Q.; Wang, W.; Lu, L.; Liu, M.; Li, J.; Yang, S.; Sun, Y.; Zhang, K.; Xu, J. Utilizations of agricultural waste as adsorbent for the removal of contaminants: A review. *Chemosphere* **2018**, *211*, 235–253. [CrossRef]
18. Chen, T.; Zhou, Z.; Xu, S.; Wang, H.; Lu, W. Adsorption behavior comparison of trivalent and hexavalent chromium on biochar derived from municipal sludge. *Bioresour. Technol.* **2015**, *190*, 388–394. [CrossRef]
19. Heng, K.S.; Hatti-Kaul, R.; Adam, F.; Fukui, T.; Sudesh, K. Conversion of rice husks to polyhydroxyalkanoates (PHA) via a three-step process: Optimized alkaline pretreatment, enzymatic hydrolysis, and biosynthesis by Burkholderia cepacia USM (JCM 15050). *J. Chem. Technol. Biotechnol.* **2017**, *92*, 100–108. [CrossRef]
20. Hesami, S.M.; Zilouei, H.; Karimi, K.; Asadinezhad, A. Enhanced biogas production from sunflower stalks using hydrothermal and organosolv pretreatment. *Ind. Crops Prod.* **2015**, *76*, 449–455. [CrossRef]
21. Katsimpouras, C.; Christakopoulos, P.; Topakas, E. Acetic acid-catalyzed hydrothermal pretreatment of corn stover for the production of bioethanol at high-solids content. *Bioprocess Biosyst. Eng.* **2016**, *39*, 1415–1423. [CrossRef] [PubMed]
22. Robl, D.; dos Santos Costa, P.; Rabelo, S.C.; da Silva Delabona, P.; da Silva Lima, D.J.; Padilla, G.; da Cruz Pradella, J.G. Use of ascomycete extracts in enzymatic cocktail formulations increases sugar cane bagasse hydrolysis. *BioEnergy Res.* **2016**, *9*, 559–565. [CrossRef]
23. Rohowsky, B.; Häßler, T.; Gladis, A.; Remmele, E.; Schieder, D.; Faulstich, M. Feasibility of simultaneous saccharification and juice co-fermentation on hydrothermal pretreated sweet sorghum bagasse for ethanol production. *Appl. Energy* **2013**, *102*, 211–219. [CrossRef]
24. Zhang, Q.; Huang, H.; Han, H.; Qiu, Z.; Achal, V. Stimulatory effect of in-situ detoxification on bioethanol production by rice straw. *Energy* **2017**, *135*, 32–39. [CrossRef]
25. Wang, L.; Yang, M.; Fan, X.; Zhu, X.; Xu, T.; Yuan, Q. An environmentally friendly and efficient method for xylitol bioconversion with high-temperature-steaming corncob hydrolysate by adapted Candida tropicalis. *Process Biochem.* **2011**, *46*, 1619–1626. [CrossRef]
26. Ahmad, F.; Zhu, D.; Sun, J. Environmental fate of tetracycline antibiotics: Degradation pathway mechanisms, challenges, and perspectives. *Environ. Sci. Eur.* **2021**, *33*, 64. [CrossRef]
27. Nii, T.; Ishii, F. Dialkylphosphatidylcholine and egg yolk lecithin for emulsification of various triglycerides. *Colloids Surf. B: Biointerfaces* **2005**, *41*, 305–311. [CrossRef]
28. Liu, X.; Shao, Z.; Wang, Y.; Liu, Y.; Wang, S.; Gao, F.; Dai, Y. New use for Lentinus edodes bran biochar for tetracycline removal. *Environ. Res.* **2023**, *216*, 114651. [CrossRef]
29. Hao, D.; Chen, Y.; Zhang, Y.; You, N. Nanocomposites of zero-valent iron@ biochar derived from agricultural wastes for adsorptive removal of tetracyclines. *Chemosphere* **2021**, *284*, 131342. [CrossRef]
30. Zhang, D.; He, Q.; Hu, X.; Zhang, K.; Chen, C.; Xue, Y. Enhanced adsorption for the removal of tetracycline hydrochloride (TC) using ball-milled biochar derived from crayfish shell. *Colloids Surf. A Physicochem. Eng. Asp.* **2021**, *615*, 126254. [CrossRef]
31. Wang, J.-S.; Yi, X.-H.; Xu, X.; Ji, H.; Alanazi, A.M.; Wang, C.-C.; Zhao, C.; Kaneti, Y.V.; Wang, P.; Liu, W. Eliminating tetracycline antibiotics matrix via photoactivated sulfate radical-based advanced oxidation process over the immobilized MIL-88A: Batch and continuous experiments. *Chem. Eng. J.* **2022**, *431*, 133213. [CrossRef]

32. Tang, X.; Huang, Y.; He, Q.; Wang, Y.; Zheng, H.; Hu, Y. Adsorption of tetracycline antibiotics by nitrilotriacetic acid modified magnetic chitosan-based microspheres from aqueous solutions. *Environ. Technol. Innov.* **2021**, *24*, 101895. [CrossRef]
33. Zhu, X.; Wan, Z.; Tsang, D.C.; He, M.; Hou, D.; Su, Z.; Shang, J. Machine learning for the selection of carbon-based materials for tetracycline and sulfamethoxazole adsorption. *Chem. Eng. J.* **2021**, *406*, 126782. [CrossRef]
34. Wang, H.; Lou, X.; Hu, Q.; Sun, T. Adsorption of antibiotics from water by using Chinese herbal medicine residues derived biochar: Preparation and properties studies. *J. Mol. Liq.* **2021**, *325*, 114967. [CrossRef]
35. Hoslett, J.; Ghazal, H.; Katsou, E.; Jouhara, H. The removal of tetracycline from water using biochar produced from agricultural discarded material. *Sci. Total Environ.* **2021**, *751*, 141755. [CrossRef]
36. Lu, L.; Liu, M.; Chen, Y.; Luo, Y. Effective removal of tetracycline antibiotics from wastewater using practically applicable iron (III)-loaded cellulose nanofibres. *R. Soc. Open Sci.* **2021**, *8*, 210336. [CrossRef]
37. Tomczyk, A.; Szewczuk-Karpisz, K. Effect of biochar modification by vitamin c, hydrogen peroxide or silver nanoparticles on its physicochemistry and tetracycline removal. *Materials* **2022**, *15*, 5379. [CrossRef]
38. Qin, Y.; Chai, B.; Wang, C.; Yan, J.; Fan, G.; Song, G. Removal of tetracycline onto KOH-activated biochar derived from rape straw: Affecting factors, mechanisms and reusability inspection. *Colloids Surf. A Physicochem. Eng. Asp.* **2022**, *640*, 128466. [CrossRef]
39. Cela-Dablanca, R.; Barreiro, A.; Rodríguez-López, L.; Santás-Miguel, V.; Arias-Estévez, M.; Fernández-Sanjurjo, M.J.; Álvarez-Rodríguez, E.; Núñez-Delgado, A. Amoxicillin Retention/Release in Agricultural Soils Amended with Different Bio-Adsorbent Materials. *Materials* **2022**, *15*, 3200. [CrossRef]
40. Yazidi, A.; Atrous, M.; Soetaredjo, F.E.; Sellaoui, L.; Ismadji, S.; Erto, A.; Bonilla-Petriciolet, A.; Dotto, G.L.; Lamine, A.B. Adsorption of amoxicillin and tetracycline on activated carbon prepared from durian shell in single and binary systems: Experimental study and modeling analysis. *Chem. Eng. J.* **2020**, *379*, 122320. [CrossRef]
41. Daouda, M.M.A.; Ońesime Akowanou, A.V.; Mahunon, S.R.; Adjinda, C.K.; Aina, M.P.; Drogui, P. Optimal removal of diclofenac and amoxicillin by activated carbon prepared from coconut shell through response surface methodology. *S. Afr. J. Chem. Eng.* **2021**, *38*, 78–89. [CrossRef]
42. Hashemzadeh, F.; Ariannezhad, M.; Derakhshandeh, S.H. Evaluation of Cephalexin and Amoxicillin removal from aqueous media using activated carbon produced from Aloe vera leaf waste. *Chem. Phys. Lett.* **2022**, *800*, 139656. [CrossRef]
43. Li, X.; Jiang, Y.; Chen, T.; Zhao, P.; Niu, S.; Yuan, M.; Ma, X. Adsorption of norfloxacin from wastewater by biochar with different substrates. *Environ. Geochem. Health* **2022**, 1–14. [CrossRef]
44. Niu, X.; Liu, C.; Li, L.; Han, X.; Chang, C.; Li, P.; Chen, J. High specific surface area N-doped activated carbon from hydrothermal carbonization of shaddock peel for the removal of norfloxacin from aqueous solution. *Water Sci. Technol.* **2022**, *85*, 2964–2979. [CrossRef] [PubMed]
45. Fang, N.; He, Q.; Sheng, L.; Xi, Y.; Zhang, L.; Liu, H.; Cheng, H. Toward broader applications of iron ore waste in pollution control: Adsorption of norfloxacin. *J. Hazard. Mater.* **2021**, *418*, 126273. [CrossRef] [PubMed]
46. Nguyen, V.-T.; Nguyen, T.-B.; Dat, N.D.; Huu, B.T.; Nguyen, X.-C.; Tran, T.; Bui, M.-H.; Dong, C.-D.; Bui, X.-T. Adsorption of norfloxacin from aqueous solution on biochar derived from spent coffee ground: Master variables and response surface method optimized adsorption process. *Chemosphere* **2022**, *288*, 132577. [CrossRef] [PubMed]
47. Zhang, Y.; Cheng, L.; Ji, Y. A novel amorphous porous biochar for adsorption of antibiotics: Adsorption mechanism analysis via experiment coupled with theoretical calculations. *Chem. Eng. Res. Des.* **2022**, *186*, 362–373. [CrossRef]
48. Zhang, M.; Zhang, K.; Wang, J.; Zhou, R.; Li, J.; Zhao, W. Study on optimal adsorption conditions of norfloxacin in water based on response surface methodology. *Water Supply* **2022**, *22*, 3661–3672. [CrossRef]
49. Zhou, H.; Wang, Z.; Gao, C.; Sun, Q.; Liu, J.; She, D. Synthesis of honeycomb lignin-based biochar and its high-efficiency adsorption of norfloxacin. *Bioresour. Technol.* **2023**, *369*, 128402. [CrossRef]
50. Chen, A.; Pang, J.; Wei, X.; Chen, B.; Xie, Y. Fast one-step preparation of porous carbon with hierarchical oxygen-enriched structure from waste lignin for chloramphenicol removal. *Environ. Sci. Pollut. Res.* **2021**, *28*, 27398–27410. [CrossRef]
51. Nguyen, L.M.; Nguyen, N.T.T.; Nguyen, T.T.T.; Nguyen, T.T.; Nguyen, D.T.C.; Tran, T.V. Occurrence, toxicity and adsorptive removal of the chloramphenicol antibiotic in water: A review. *Environ. Chem. Lett.* **2022**, *20*, 1929–1963. [CrossRef] [PubMed]
52. Falyouna, O.; Maamoun, I.; Ghosh, S.; Malloum, A.; Othmani, A.; Eljamal, O.; Amen, T.W.; Oroke, A.; Bornman, C.; Ahmadi, S. Sustainable Technologies for the Removal of Chloramphenicol from Pharmaceutical Industries Effluent: A critical review. *J. Mol. Liq.* **2022**, *368*, 120726. [CrossRef]
53. Khelifa, M.; Mellouk, S.; Lecomte-Nana, G.L.; Batonneau-Gener, I.; Marouf-Khelifa, K.; Khelifa, A. Methodological approach to the chloramphenicol adsorption by acid-leached halloysites: Preparation, characterization, performance and mechanism. *Microporous Mesoporous Mater.* **2023**, *348*, 112412. [CrossRef]
54. Wang, G.; Yong, X.; Luo, L.; Yan, S.; Wong, J.W.; Zhou, J. Structure-performance correlation of high surface area and hierarchical porous biochars as chloramphenicol adsorbents. *Sep. Purif. Technol.* **2022**, *296*, 121374. [CrossRef]
55. Xing, W.; Liu, Q.; Wang, J.; Xia, S.; Ma, L.; Lu, R.; Zhang, Y.; Huang, Y.; Wu, G. High selectivity and reusability of biomass-based adsorbent for chloramphenicol removal. *Nanomaterials* **2021**, *11*, 2950. [CrossRef]
56. Pasta, P.C.; Silva, A.C.; Jorgetto, A.O.; Saeki, M.J.; Pedrosa, V.d.A.; Martines, M.A.; Schneider, J.F.; Minatel, I.O.; Rabelo, J.; Castro, R.S. Use of Typha angustifolia L. as biosorbent to remove chloramphenicol in aqueous samples. *Eur. J. Adv. Chem. Res.* **2022**, *3*, 64–86. [CrossRef]

57. Zhu, H.; Qiu, J.; Zhou, D.; Wang, H.; Xu, D.; Li, H. Synthesis of coconut fiber activated carbon for chloramphenicol wastewater adsorption. *Res. Chem. Intermed.* **2022**, *48*, 3613–3631. [CrossRef]
58. Geng, X.; Lv, S.; Yang, J.; Cui, S.; Zhao, Z. Carboxyl-functionalized biochar derived from walnut shells with enhanced aqueous adsorption of sulfonamide antibiotics. *J. Environ. Manag.* **2021**, *280*, 111749. [CrossRef]
59. Xu, T.; Du, J.; Zhang, J.; David, W.; Liu, P.; Faheem, M.; Zhu, X.; Yang, J.; Bao, J. Microbially-mediated synthesis of activated carbon derived from cottonseed husks for enhanced sulfanilamide removal. *J. Hazard. Mater.* **2022**, *426*, 127811. [CrossRef]
60. Prasannamedha, G.; Kumar, P.S.; Mehala, R.; Sharumitha, T.; Surendhar, D. Enhanced adsorptive removal of sulfamethoxazole from water using biochar derived from hydrothermal carbonization of sugarcane bagasse. *J. Hazard. Mater.* **2021**, *407*, 124825. [CrossRef]
61. Qin, P.; Huang, D.; Tang, R.; Gan, F.; Guan, Y.; Lv, X. Enhanced adsorption of sulfonamide antibiotics in water by modified biochar derived from bagasse. *Open Chem.* **2019**, *17*, 1309–1316. [CrossRef]
62. Aslan, S.; Şirazi, M. Adsorption of sulfonamide antibiotic onto activated carbon prepared from an agro-industrial by-product as low-cost adsorbent: Equilibrium, thermodynamic, and kinetic studies. *Water Air Soil Pollut.* **2020**, *231*, 1–20. [CrossRef]
63. Weng, M.; Yu, X. Electrochemical oxidation of para-aminophenol with rare earth doped lead dioxide electrodes: Kinetics modeling and mechanism. *Front. Chem.* **2019**, *7*, 382. [CrossRef]
64. Hu, J.; Liu, F.; Shan, Y.; Huang, Z.; Gao, J.; Jiao, W. Enhanced Adsorption of Sulfonamides by Attapulgite-Doped Biochar Prepared with Calcination. *Molecules* **2022**, *27*, 8076. [CrossRef] [PubMed]
65. Sun, Y.; Zheng, L.; Zheng, X.; Xiao, D.; Yang, Y.; Zhang, Z.; Ai, B.; Sheng, Z. Adsorption of sulfonamides in aqueous solution on reusable coconut-shell biochar modified by alkaline activation and magnetization. *Front. Chem.* **2022**, *9*, 1274. [CrossRef]
66. Correa-Navarro, Y.M.; Giraldo, L.; Moreno-Piraján, J.C. Biochar from fique bagasse for remotion of caffeine and diclofenac from aqueous solution. *Molecules* **2020**, *25*, 1849. [CrossRef] [PubMed]
67. Malesic-Eleftheriadou, N.; Liakos, E.V.; Evgenidou, E.; Kyzas, G.Z.; Bikiaris, D.N.; Lambropoulou, D.A. Low-cost agricultural wastes (orange peels) for the synthesis and characterization of activated carbon biosorbents in the removal of pharmaceuticals in multi-component mixtures from aqueous matrices. *J. Mol. Liq.* **2022**, *368*, 120795. [CrossRef]
68. de Souza, R.M.; Quesada, H.B.; Cusioli, L.F.; Fagundes-Klen, M.R.; Bergamasco, R. Adsorption of non-steroidal anti-inflammatory drug (NSAID) by agro-industrial by-product with chemical and thermal modification: Adsorption studies and mechanism. *Ind. Crops Prod.* **2021**, *161*, 113200. [CrossRef]
69. Bouhcain, B.; Carrillo-Peña, D.; El Mansouri, F.; Ez Zoubi, Y.; Mateos, R.; Morán, A.; Quiroga, J.M.; Zerrouk, M.H. Removal of emerging contaminants as diclofenac and caffeine using activated carbon obtained from argan fruit shells. *Appl. Sci.* **2022**, *12*, 2922. [CrossRef]
70. Alvear-Daza, J.J.; Cánneva, A.; Donadelli, J.A.; Manrique-Holguín, M.; Rengifo-Herrera, J.A.; Pizzio, L.R. Removal of diclofenac and ibuprofen on mesoporous activated carbon from agro-industrial wastes prepared by optimized synthesis employing a central composite design. *Biomass Convers. Biorefinery* **2022**, 1–23. [CrossRef]
71. Viotti, P.V.; Moreira, W.M.; dos Santos, O.A.A.; Bergamasco, R.; Vieira, A.M.S.; Vieira, M.F. Diclofenac removal from water by adsorption on Moringa oleifera pods and activated carbon: Mechanism, kinetic and equilibrium study. *J. Clean. Prod.* **2019**, *219*, 809–817. [CrossRef]
72. Malhotra, M.; Suresh, S.; Garg, A. Tea waste derived activated carbon for the adsorption of sodium diclofenac from wastewater: Adsorbent characteristics, adsorption isotherms, kinetics, and thermodynamics. *Environ. Sci. Pollut. Res.* **2018**, *25*, 32210–32220. [CrossRef] [PubMed]
73. Avcu, T.; Üner, O.; Geçgel, Ü. Adsorptive removal of diclofenac sodium from aqueous solution onto sycamore ball activated carbon–isotherms, kinetics, and thermodynamic study. *Surf. Interfaces* **2021**, *24*, 101097. [CrossRef]
74. Karadeniz, F.; Güzel, F. Adsorptive performance of Melia Azedarach fruit-derived biochar in removing methylene blue, diclofenac, and copper (II) from aqueous solution. *Biomass Convers. Biorefinery* **2022**, *13*, 2429–2447. [CrossRef]
75. Abadian, S.; Shayesteh, H.; Rahbar-Kelishami, A. Effective adsorption of diclofenac sodium from aqueous solution using cationic surfactant modified Cuminum cyminum agri-waste: Kinetic, equilibrium, and thermodynamic studies. *Int. J. Phytoremediat.* **2022**, 1–11. [CrossRef] [PubMed]
76. Shin, J.; Kwak, J.; Lee, Y.-G.; Kim, S.; Choi, M.; Bae, S.; Lee, S.-H.; Park, Y.; Chon, K. Competitive adsorption of pharmaceuticals in lake water and wastewater effluent by pristine and NaOH-activated biochars from spent coffee wastes: Contribution of hydrophobic and π-π interactions. *Environ. Pollut.* **2021**, *270*, 116244. [CrossRef]
77. Matějová, L.; Bednárek, J.; Tokarský, J.; Koutník, I.; Sokolová, B.; Cruz, G.J.F. Adsorption of the most common non-steroidal analgesics from aquatic environment on agricultural wastes-based activated carbons; experimental adsorption study supported by molecular modeling. *Appl. Surf. Sci.* **2022**, *605*, 154607. [CrossRef]
78. Costa, R.L.T.; do Nascimento, R.A.; de Araújo, R.C.S.; Vieira, M.G.A.; da Silva, M.G.C.; de Carvalho, S.M.L.; de Faria, L.J.G. Removal of non-steroidal anti-inflammatory drugs (NSAIDs) from water with activated carbons synthetized from waste murumuru (Astrocaryum murumuru Mart.): Characterization and adsorption studies. *J. Mol. Liq.* **2021**, *343*, 116980. [CrossRef]
79. Arinkoola, A.; Alagbe, S.; Akinwole, I.; Ogundiran, A.; Ajayi, L.; Agbede, O.; Ogunleye, O. Adsorptive Removal of Ibuprofen, Ketoprofen and Naproxen from Aqueous Solution Using Coconut Shell Biomass. *Environ. Res. Eng. Manag.* **2022**, *78*, 28–37. [CrossRef]

80. Kebede, T.; Dube, S.; Nindi, M. Removal of non-steroidal anti-inflammatory drugs (NSAIDs) and carbamazepine from wastewater using water-soluble protein extracted from Moringa stenopetala seeds. *J. Environ. Chem. Eng.* **2018**, *6*, 3095–3103. [CrossRef]
81. Franco, D.S.; Pinto, D.; Georgin, J.; Netto, M.S.; Foletto, E.L.; Manera, C.; Godinho, M.; Silva, L.F.; Dotto, G.L. Conversion of Erythrina speciosa pods to porous adsorbent for Ibuprofen removal. *J. Environ. Chem. Eng.* **2022**, *10*, 108070. [CrossRef]
82. Oba, S.N.; Ighalo, J.O.; Aniagor, C.O.; Igwegbe, C.A. Removal of ibuprofen from aqueous media by adsorption: A comprehensive review. *Sci. Total Environ.* **2021**, *780*, 146608. [CrossRef] [PubMed]
83. Danil de Namor, A.; Al Nuaim, M.; Fairclough, G.; Khalife, R.; Al Hakawati, N. Amine-modified silica for removing aspirin from water. *Int. J. Environ. Sci. Technol.* **2022**, *19*, 4143–4152. [CrossRef]
84. Zhe, W.; Wenjuan, Z.; Haihan, W.; Zhiwei, W.; Jing, C. Oxidation of acetylsalicylic acid in water by UV/O3 process: Removal, byproduct analysis, and investigation of degradation mechanism and pathway. *J. Environ. Chem. Eng.* **2021**, *9*, 106259. [CrossRef]
85. N'diaye, A.D.; Kankou, M.S.A. Adsorption of aspirin onto biomaterials from aqueous solutions. *Cellulose* **2020**, *11*, 41–43.
86. Al-Sareji, O.J.; Meiczinger, M.; Salman, J.M.; Al-Juboori, R.A.; Hashim, K.S.; Somogyi, V.; Jakab, M. Ketoprofen and aspirin removal by laccase immobilized on date stones. *Chemosphere* **2023**, *311*, 137133. [CrossRef] [PubMed]
87. Wong, S.; Lee, Y.; Ngadi, N.; Inuwa, I.M.; Mohamed, N.B. Synthesis of activated carbon from spent tea leaves for aspirin removal. *Chin. J. Chem. Eng.* **2018**, *26*, 1003–1011. [CrossRef]
88. Romano, N.C.; Tentler Prola, L.D.; Passig, F.H.; Freire, F.B.; Ferreira, R.C.; Vinicius de Liz, M.; Querne de Carvalho, K. Thermal treated sugarcane bagasse for acetylsalicylic acid removal: Dynamic and equilibrium studies, cycles of reuse and mechanisms. *Int. J. Environ. Anal. Chem.* **2022**, 1–17. [CrossRef]
89. N'diaye, A.D.; Kankou, M.S.A. Sorption of Aspirin from Aqueous Solutions using Rice Husk as Low Cost Sorbent. *J. Environ. Treat. Tech.* **2020**, *8*, 1–5.
90. Laali, K.K.; Greves, W.J.; Correa-Smits, S.J.; Zwarycz, A.T.; Bunge, S.D.; Borosky, G.L.; Manna, A.; Paulus, A.; Chanan-Khan, A. Novel fluorinated curcuminoids and their pyrazole and isoxazole derivatives: Synthesis, structural studies, Computational/Docking and in-vitro bioassay. *J. Fluor. Chem.* **2018**, *206*, 82–98. [CrossRef]
91. Tutak, M.; Brodny, J. Determination of particular endogenous fires hazard zones in goaf with caving of longwall. *IOP Conf. Ser. Earth Environ. Sci.* **2017**, *95*, 042026. [CrossRef]
92. Georgin, J.; Franco, D.S.; da Boit Martinello, K.; Lima, E.C.; Silva, L.F. A review of the toxicology presence and removal of ketoprofen through adsorption technology. *J. Environ. Chem. Eng.* **2022**, *10*, 107798. [CrossRef]
93. Yanan, C.; Ali, J.; Sellaoui, L.; Dhaouadi, F.; Naeem, M.; Franco, D.S.; Georgin, J.; Erto, A.; Badawi, M. Explaining the adsorption mechanism of the herbicide 2, 4-D and the drug ketoprofen onto wheat husks Fagopyrum esculentum treated with H_2SO_4. *Chemosphere* **2023**, *313*, 137355. [CrossRef]
94. Georgin, J.; Yamil, L.d.O.; Franco, D.S.; Netto, M.S.; Piccilli, D.G.; Perondi, D.; Silva, L.F.; Foletto, E.L.; Dotto, G.L. Development of highly porous activated carbon from Jacaranda mimosifolia seed pods for remarkable removal of aqueous-phase ketoprofen. *J. Environ. Chem. Eng.* **2021**, *9*, 105676. [CrossRef]
95. Dhaouadi, F.; Sellaoui, L.; Taamalli, S.; Louis, F.; El Bakali, A.; Badawi, M.; Georgin, J.; Franco, D.S.; Silva, L.F.; Bonilla-Petriciolet, A. Enhanced adsorption of ketoprofen and 2, 4-dichlorophenoxyactic acid on Physalis peruviana fruit residue functionalized with H_2SO_4: Adsorption properties and statistical physics modeling. *Chem. Eng. J.* **2022**, *445*, 136773. [CrossRef]
96. Preigschadt, I.A.; Bevilacqua, R.C.; Netto, M.S.; Georgin, J.; Franco, D.S.; Mallmann, E.S.; Pinto, D.; Foletto, E.L.; Dotto, G.L. Optimization of ketoprofen adsorption from aqueous solutions and simulated effluents using H_2SO_4 activated Campomanesia guazumifolia bark. *Environ. Sci. Pollut. Res.* **2022**, *29*, 2122–2135. [CrossRef]
97. Fadzail, F.; Hasan, M.; Mokhtar, Z.; Ibrahim, N.; An, O.; Abidin, C. Batch adsorption studies for ketoprofen removal via Dillenia Indica peel activated carbon. *IOP Conf. Ser. Earth Environ. Sci.* **2021**, *920*, 012010. [CrossRef]
98. Franco, D.S.; Georgin, J.; Netto, M.S.; da Boit Martinello, K.; Silva, L.F. Preparation of activated carbons from fruit residues for the removal of naproxen (NPX): Analytical interpretation via statistical physical model. *J. Mol. Liq.* **2022**, *356*, 119021. [CrossRef]
99. Paunovic, O.; Pap, S.; Maletic, S.; Taggart, M.A.; Boskovic, N.; Sekulic, M.T. Ionisable emerging pharmaceutical adsorption onto microwave functionalised biochar derived from novel lignocellulosic waste biomass. *J. Colloid Interface Sci.* **2019**, *547*, 350–360. [CrossRef]
100. Georgin, J.; da Boit Martinello, K.; Franco, D.S.; Netto, M.S.; Piccilli, D.G.; Foletto, E.L.; Silva, L.F.; Dotto, G.L. Efficient removal of naproxen from aqueous solution by highly porous activated carbon produced from Grapetree (Plinia cauliflora) fruit peels. *J. Environ. Chem. Eng.* **2021**, *9*, 106820. [CrossRef]
101. Georgin, J.; Netto, M.S.; Franco, D.S.; Piccilli, D.G.; da Boit Martinello, K.; Silva, L.F.; Foletto, E.L.; Dotto, G.L. Woody residues of the grape production chain as an alternative precursor of high porous activated carbon with remarkable performance for naproxen uptake from water. *Environ. Sci. Pollut. Res.* **2022**, *29*, 16988–17000. [CrossRef] [PubMed]
102. Fadzail, F.; Hasan, M.; Mokhtar, Z.; Ibrahim, N. Removal of naproxen using low-cost Dillenia Indica peels as an activated carbon. *Mater. Today Proc.* **2022**, *57*, 1108–1115. [CrossRef]
103. Wang, L.; Shi, C.; Pan, L.; Zhang, X.; Zou, J.-J. Rational design, synthesis, adsorption principles and applications of metal oxide adsorbents: A review. *Nanoscale* **2020**, *12*, 4790–4815. [CrossRef] [PubMed]
104. Singh, S.; Kumar, V.; Anil, A.G.; Kapoor, D.; Khasnabis, S.; Shekar, S.; Pavithra, N.; Samuel, J.; Subramanian, S.; Singh, J. Adsorption and detoxification of pharmaceutical compounds from wastewater using nanomaterials: A review on mechanism, kinetics, valorization and circular economy. *J. Environ. Manag.* **2021**, *300*, 113569. [CrossRef]

105. Patel, M.; Kumar, R.; Pittman, C.U., Jr.; Mohan, D. Ciprofloxacin and acetaminophen sorption onto banana peel biochars: Environmental and process parameter influences. *Environ. Res.* **2021**, *201*, 111218. [CrossRef]
106. Rivas, B.L.; Oñate, P.; Palacio, D.A. Removal of oxytetracycline by polymers. an overview. *J. Chil. Chem. Soc.* **2020**, *65*, 4943–4947. [CrossRef]
107. Liu, Z.; Zhou, Q.; Zhao, B.; Li, S.; Xiong, Y.; Xu, W. Few-layer N-doped porous carbon nanosheets derived from corn stalks as a bifunctional electrocatalyst for overall water splitting. *Fuel* **2020**, *280*, 118567. [CrossRef]
108. Oberoi, A.S.; Jia, Y.; Zhang, H.; Khanal, S.K.; Lu, H. Insights into the fate and removal of antibiotics in engineered biological treatment systems: A critical review. *Environ. Sci. Technol.* **2019**, *53*, 7234–7264. [CrossRef]